Effects of double-layer polarization and counterion condensation on the electrophoresis of polyelectrolytes

ARTICLE *in* SOFT MATTER · JANUARY 2011

Impact Factor: 4.03 · DOI: 10.1039/C0SM00600A

Effects of double-layer polarization and counterion condensation on the electrophoresis of polyelectrolytes

Li-Hsien Yeh and Jyh-Ping Hsu*

Received 30th June 2010, Accepted 26th August 2010
DOI: 10.1039/c0sm00600a

The electrophoretic behavior of an entirely porous, charged entity such as DNA, protein, or a synthetic polymer is modeled. Adopting a spherical polyelectrolyte on the axis of a narrow, long cylindrical pore as the model system, we show that, in addition to the effects of boundary, double-layer polarization arising from the deformation of the ionic cloud surrounding the polyelectrolyte due to the convective flow of ionic species, and electroosmotic retardation flow coming from the motion of unbalanced amount of counterions in the double layer, the effect of counterion condensation also plays a role, yielding behaviors that are different both quantitatively and qualitatively with those of the corresponding rigid and soft particles. The present analysis predicts the presence of several unexpected and interesting results. For instance, the electrophoretic mobility of the polyelectrolyte may show a local maximum as the amount of its fixed charge varies, and the amount of fixed charge at which the local maximum occurs depends upon the thickness of double layer, the relative size of the pore, and the friction coefficient of the polyelectrolyte. These findings are consistent with the experimental observations in the literature, but the relevant mechanisms have not been proposed and/or explained satisfactorily. The results gathered in this study provide valuable information for both the design of an electrophoresis apparatus and the interpretation of experimental data.

1. Introduction

A charged colloidal particle in an electrolyte solution can be driven by an applied electric field, known as electrophoresis. For an isolated, rigid, spherical, non-conducting particle of constant surface (zeta) potential ζ in an infinite, Newtonian electrolyte solution of dielectric constant ε and viscosity η, von Smoluchowski[1] was able to show that, under the conditions of high electrolyte concentration, the application of an electric field of strength E yields

$$\mu = \frac{U_p}{E} = \frac{\varepsilon\zeta}{\eta} \quad (1)$$

where U_p and μ are the electrophoretic velocity and the electrophoretic mobility of the particle, respectively. The straightforward and concise nature of eqn (1) makes it readily applicable both in the design of an electrophoresis apparatus and the interpretation of experimental data.

Since the pioneer theoretical analysis of von Smoluchowski, electrophoresis has been studied extensively by many researchers to account for conditions that are of more practical significance. These include, for example, Hückel,[2] Henry,[3] Overbeek,[4] Booth,[5] O'Brien and White,[6] and Ohshima *et al.*[7] Most of these studies focused on rigid particles where its surface is impenetrable to the surrounding ionic species and the liquid medium. In practice, a wide range of colloidal particles do not have this nature. For example, soft or fuzzy particles,[8–13] which consist of a rigid core and an ion-penetrable membrane or polymer layer, should not be treated as rigid. In general, the electrophoretic behavior of a soft particle is more complicated than that of the corresponding rigid particle because the membrane layer of the former can influence appreciably both the electric and the flow fields near its surface.[14–17] The problem becomes more complicated if the membrane layer is charged because the effect of double-layer polarization (DLP), one of the interesting and important effects of electrophoresis, can be significant when the surface potential is high.[18–22] That effect, which usually retards the particle motion,[6,22] comes from the convective motion of the ionic species inside double layer, and is most important when the thickness of double layer is comparable to the particle size.[6] Saville[18] and Hill *et al.*[19] investigated the electrophoresis of an isolated soft spherical particle in an infinite electrolyte medium taking the effect of DLP into account. Lee *et al.*[20] extended their analysis to the case of a dispersion of soft particles under the conditions of high surface potential. The electrophoresis of a soft particle in an uncharged spherical cavity was investigated by Lee *et al.*,[21] and that normal to a large plane by Cheng *et al.*[22] Under the conditions of weak applied electric field and low surface potential, Ohshima[23–25] derived several approximate analytical formulas for the electrophoretic mobility of soft particles, which are readily applicable to experimentalists.

Entirely porous particles such as polyelectrolytes[13,26–28] and polymer gels[13,28–30] are another important class of colloidal particles. Many organic and biological entities, for example, proteins, DNA, and microorganisms, belong to this category. Although a porous particle can be viewed as the limiting case of a soft particle where its rigid core is infinitely small, a remarkable difference between the two is that the concept of zeta potential is inapplicable in the former. That is, the electrokinetic behavior of a porous particle depends only on its physical properties such as

Department of Chemical Engineering, National Taiwan University, Taipei, Taiwan 10617. E-mail: jphsu@ntu.edu.tw; Fax: +886-2-23623040; Tel: +886-2-23637448

the amount of fixed charge, thereby yielding electrophoretic behavior that is different both quantitatively and qualitatively from that of a rigid particle.[31–38] Due to the dissociation of the functional groups of its bone segments, a polyelectrolyte is charged once immersed in an electrolyte solution. Assuming low electric potential (DLP is unimportant) Hermans and Fujita[31,32] analyzed theoretically the electrophoresis of an isolated charged porous sphere (or spherical polyelectrolyte) in an infinite electrolyte medium by adopting Brinkman equation[33,34] to describe the flow field inside the sphere. Under the conditions of high electrolyte concentration (large Debye screening length, κ^{-1}) and constant fixed charged density ρ_{fix}, it was shown that[32]

$$\mu = \frac{\rho_{fix}}{\eta\lambda^2}\left[1 + \frac{2}{3}\left(\frac{\lambda}{\kappa}\right)^2 \frac{1+\lambda/2\kappa}{1+\lambda/\kappa}\right] \tag{2}$$

where $\lambda = (\gamma/\eta)^{1/2}$ with γ being the frictional coefficient of the polyelectrolyte. A comparison between eqn (1) and (2) reveals that the mobility of a rigid particle correlates with its zeta potential but that of a porous particle with its fixed charge density. In the latter, counterions are attracted into the polyelectrolyte and co-ions are expelled out, resulting in a non-uniform ionic distribution both inside and outside the polyelectrolyte. Therefore, the conventional concept of zeta potential for a rigid particle becomes inapplicable for a porous particle (or polyelectrolyte), implying that the concept of double layer in the former needs be modified accordingly.[28–32] Eqn (2) was also derived by Overbeek and Stigter.[35] Taking the effect of DLP, Imai and Iwasa[36] analyzed the electrophoresis of a nearly free-drained polyelectrolytes by adopting a cubic free volume model.[37] It was found that the applied electric field near the polyelectrolytes was strongly depressed by the counterions, and this result agrees well with the experimental data. In a study of the electrophoresis of a concentrated dispersion of charged porous spheres under the conditions of arbitrary fixed charged density and double layer thickness, He and Lee[38] concluded that the higher the fixed charged density the more significant the effect DLP is.

Both eqn (1) and (2) are based on an isolated particle in an infinite fluid. These conditions can be unrealistic in practice. The presence of nearby particles, for example, can be significant if the concentration of particles is appreciable, and if electrophoresis is conducted in a narrow space, such as in capillary electrophoresis, the boundary effect should be considered. In the latter, care must be taken in the interpretation of the experimental data because the electrophoretic mobility of a particle can be influenced both quantitatively and qualitatively by a boundary. The boundary effect on electrophoresis has been studied by many researchers in the past decades by considering both rigid particles[39–52] and soft particles[16,17,21,22] in various types of problem. These include, for example, a sphere normal to a plane[22,39–41] or in a spherical cavity,[21,42,43] and a sphere,[16,17,39,40,44–47] a cylinder,[48–50] an ellipsoid,[51] and two spheres[52] in a cylindrical pore.

Recently, Hsu *et al.*[16] and Zhang *et al.*[17] modeled theoretically the electrophoresis of a soft sphere along the axis of a cylindrical pore. Because they assumed that the surface potential is low, a linearized Poisson–Boltzmann equation[23–25] is applicable to the description of the electrical potential. That assumption, although simplifies drastically the relevant analyses, is unable to take account of the effect of DLP.[53] Although the effect of DLP was considered by Hsu and Chen[46] in a study of the electrophoresis of a rigid sphere along the axis of a cylindrical pore, the nature of the particle assumed makes it unable to describe a wide class of colloidal particles with a non-rigid nature. In particular, the effect of counterion condensation,[54,55] which does not occur in the case of rigid particles, can play a role. This effect is reflected by, for example, the fact that the electrophoretic mobility of a soft particle is independent,[56,57] or nearly so,[56–58] of the total amount of charge carried by its polyelectrolyte layer when a critical charge loading is reached. The effect of counterion condensation is pronounced if a particle is entirely porous, or if it is a polyelectrolyte.[54] However, up to now, there is a lack of the available results in the literature for an entirely porous particle for the case where the effects of boundary, DLP, and counterion condensation are all present. In an attempt to extend previous analyses to this case, we consider the electrophoresis of a spherical polyelectrolyte along the axis of a cylindrical pore under the conditions of arbitrary electrical potential and double layer thickness. Typical application of the geometry considered includes, for example, the separation of protein,[59] and DNA[60] through capillary electrophoresis. The electrophoretic behaviors of the polyelectrolyte under various conditions are discussed by varying its physicochemical properties, the thickness of double layer, and the size of the pore.

2. Model

Referring to Fig. 1, we consider the electrophoresis of a spherical polyelectrolyte of radius a along the axis of a long, nonconducting cylindrical pore of radius b. Let $\Lambda = a/b$, which measures the significance of the boundary effect; the larger the value of Λ the more important the boundary effect. The polyelectrolyte carries uniformly distributed fixed charge and the pore is filled with an aqueous, incompressible Newtonian fluid containing z_1:z_2 electrolytes with z_1 and z_2 being the valences of cations and of anions, respectively, with $\alpha = -z_2/z_1$. The cylindrical coordinates, r, θ, z, with the origin at the center of the polyelectrolyte are adopted. $\mathbf{E}$ is an applied uniform electric field directed in the z-direction with strength E. The present problem is θ-symmetric and, therefore, only the (r, z) domain needs be considered.

The Reynolds number of the flow field in electrophoresis is much smaller than unity, that is, the inertial term of the equation governing the flow field can be neglected. Letting ϕ and $\mathbf{u}$ be the electric potential and the relative velocity of the fluid phase to the polyelectrolyte, respectively, the present problem can be described by

$$\nabla^2\phi = -\frac{\rho + h(r,z)\rho_{fix}}{\varepsilon} \tag{3}$$

$$\nabla\cdot\left[-D_j\left(\nabla n_j + \frac{z_j e}{k_B T} n_j \nabla\phi\right) + n_j\mathbf{u}\right] = 0 \tag{4}$$

$$\nabla\cdot\mathbf{u} = 0 \tag{5}$$

$$-\nabla p + \eta\nabla^2\mathbf{u} - \rho\nabla\phi - h(r,z)\gamma\mathbf{u} = 0 \tag{6}$$

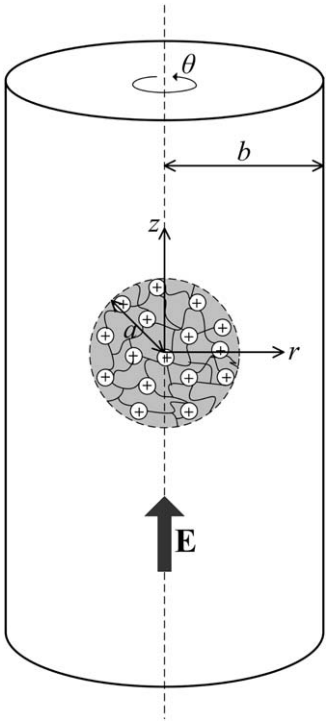

Fig. 1 Electrophoresis of a charged, porous spherical polyelectrolyte of radius a along the axis of a long, non-conducting cylindrical pore of radius b; **E** is a uniform applied electric field with direction parallel to the axis of the pore; r, θ, z are the cylindrical coordinates with the origin at the center of the polyelectrolyte.

Here, ∇^2 and ∇ are the Laplace operator and the gradient operator, respectively; $h(r,z)$ is a region function: $h(r,z) = 0$ for the region outside the polyelectrolyte layer and $h(r,z) = 1$ for the region inside the polyelectrolyte. ε, $\rho(=\sum_{j=1}^{2} z_j e n_j)$, and ρ_{fix} are the permittivity of the fluid phase, the space charge density of mobile ions, and the fixed charged density of the polyelectrolyte, respectively. D_j, n_j, and z_j are the diffusivity, the number concentration, and the valance of ionic species j, respectively. e, k_B, and T are the elementary charge, the Boltzmann constant, and the absolute temperature, respectively. η and p are the viscosity and the pressure of the fluid phase, respectively. γ is the hydrodynamic frictional coefficient of the polyelectrolyte per unit volume. Eqn (4) states that the ion species are driven not only by the flow of fluid but also by the concentration gradient and the electric field. This implies that even for the case of $\gamma \to \infty$, where the fluid flow inside the polyelectrolyte vanishes ($\mathbf{u} = \mathbf{0}$), the ionic species inside the polyelectrolyte are not stagnant. Eqn (5) and (6) are the continuity equation and a modified Navier–Stokes equation with $-\rho\nabla\phi$ and $-\gamma\mathbf{u}$ being the electric body force and the frictional force exerted on the fluid by the composing material of the polyelectrolyte.[34] For a porous polymeric particle, γ can be expressed as $6\pi\eta a_S N_S$ in the free-draining limit with a_S and N_S being the Stokes radius and the number density of the hydrodynamic frictional polymer segments, respectively.[61,62] For simplicity, we assume that the values of ε, D_j, and η inside the polyelectrolyte are the same as those outside it, and ρ_{fix} is position independent. Without loss of generality, we assume that the polyelectrolyte is positively charged.

The methodology proposed by O'Brien and White is adopted,[6] where the applied electric field is assumed to be much weaker than the electric field established by the polyelectrolyte. This assumption is appropriate when $E < 25$ kV m^{-1},[63] which is usually satisfied under conditions of practical significance. Here, the dependent variables $\mathbf{u}$, p, ϕ, n_j, and ρ are decomposed into an equilibrium term, symbol with subscript e, and a perturbed term, symbol with prefix δ, as[6,61,63] $\mathbf{u} = \mathbf{u}_e + \delta\mathbf{u}$, $p = p_e + \delta P$, $\phi = \phi_e + \delta\phi$, $n_j = n_{je} + \delta n_j$, $\rho = \rho_e + \delta\rho$. The equilibrium terms arise from the presence of the polyelectrolyte only and the perturbed terms from the application of **E**. Because the polyelectrolyte is stagnant at equilibrium, $\mathbf{u}_e = 0$,[6,61,63] that is, $\mathbf{u} = \delta\mathbf{u}$.

If the effect of DLP is significant, then the electric double layer surrounding the polyelectrolyte is no longer spherically symmetric. To take this effect into account, n_j is expressed as[6,64]

$$n_j = n_{j0}\exp\left[-\frac{z_j e(\phi_e + \delta\phi + g_j)}{k_B T}\right], \quad j = 1,2 \tag{7}$$

where g_j is a hypothetical perturbed potential and n_{j0} is the bulk number concentration of ionic species j.

Under the condition of weak applied electric field, $\phi_e \gg \delta\phi$ and $\phi_e \gg \delta\phi + g_j$. In this case, expanding eqn (7) into Taylor series and neglecting higher-order terms gives

$$n_j = n_{j0}\exp\left(-\frac{z_j e\phi_e}{k_B T}\right)\left[1 - \frac{z_j e}{k_B T}(\delta\phi + g_j)\right], \quad j = 1,2 \tag{8}$$

Then, it can be shown that the concentration and the electric fields,[38,63] and the flow field[65] can be described by

$$\nabla^{*2}\phi_e^* = -\frac{(\kappa a)^2}{1+\alpha}\left[\exp(-\phi_e^*) - \exp(\alpha\phi_e^*)\right] - h(r,z)Q_{fix} \tag{9}$$

$$\nabla^{*2}\delta\phi^* = \frac{(\kappa a)^2}{1+\alpha}\left[(\delta\phi^* + g_1^*)\exp(-\phi_e^*) + \alpha(\delta\phi^* + g_2^*)\exp(\alpha\phi_e^*)\right] \tag{10}$$

$$\nabla^{*2}g_1^* - \nabla^*\phi_e^*\cdot\nabla^* g_1^* = Pe_1\mathbf{u}^*\cdot\nabla^*\phi_e^* \tag{11}$$

$$\nabla^{*2}g_2^* + \alpha\nabla^*\phi_e^*\cdot\nabla^* g_2^* = Pe_2\mathbf{u}^*\cdot\nabla^*\phi_e^* \tag{12}$$

$$\nabla^*\cdot\mathbf{u}^* = 0 \tag{13}$$

$$-\nabla^*\delta P^* + \nabla^{*2}\mathbf{u}^* + [(\nabla^{*2}\phi_e^* + h(r,z)Q_{fix})\nabla^*\delta\phi^* + \nabla^{*2}\delta\phi^*\nabla^*\phi_e^*] - h(r,z)(\lambda a)^2\mathbf{u}^* = 0 \tag{14}$$

$$n_1^* = \exp(-\phi_e^*)[1 - (\delta\phi^* + g_1^*)] \tag{15}$$

$$n_2^* = \exp(\alpha\phi_e^*)[1 + \alpha(\delta\phi^* + g_2^*)] \tag{16}$$

Here, $\phi_e^* = \phi_e/\phi_{\mathrm{ref}}$, $\delta\phi^* = \delta\phi/\phi_{\mathrm{ref}}$, $\nabla^* = a\nabla$, $\nabla^{*2} = a^2\nabla^2$, $g_j^* = g_j/\phi_{\mathrm{ref}}$, $n_j^* = n_j/n_{j0}$, and $\mathbf{u}^* = \mathbf{u}/U_{\mathrm{ref}}$, $\delta P^* = \delta P/[\varepsilon(\phi_{\mathrm{ref}})^2/a^2]$, and $\lambda = \sqrt{\gamma/\eta}$ with $\phi_{\mathrm{ref}} = k_B T/ez_1$ and $U_{\mathrm{ref}} = \varepsilon(\phi_{\mathrm{ref}})^2/\eta a$. $\kappa = [\sum_{j=1}^{2} n_{j0}(ez_j)^2/\varepsilon k_B T]^{1/2}$ is the reciprocal Debye length; $Q_{fix} = \rho_{fix}a^2/\varepsilon\phi_{\mathrm{ref}}$ is the scaled fixed charge density of the polyelectrolyte; and $Pe_j = \varepsilon(\phi_{\mathrm{ref}})^2/\eta D_j$ is the electric Peclet

number of ionic species j, respectively. λ^{-1} is the softness parameter of the polyelectrolyte,[27] which also represents the shielding length characterizing the extent of flow penetration into the polyelectrolyte.[62] For example, in the surface region of human erythrocytes,[66] rat lymphocytes,[67] and grafted polymer microcapsules[68] in an electrolyte solution, $\lambda^{-1} \cong 3$nm.

Suppose that the pore is non-conductive, impermeable to ion species, remained at constant surface potential, and non-slip. The concentration of ionic species away from the polyelectrolyte reaches the corresponding bulk value. For convenience, we let the slipping plane, where the liquid velocity relative to the polyelectrolyte vanishes, be on the pore boundary, that is, both the pore and the bulk fluid move with a relative velocity of $-U_p^*\mathbf{e}_z$, and both the pore and the bulk fluid move with a relative velocity of $-U_p^*\mathbf{e}_z$, where $U_p^* = U_p/U_{\text{ref}}$ with U_p and $\mathbf{e}_z$ being the speed of the polyelectrolyte and the unit vector in the z-direction, respectively. Therefore, the following boundary conditions apply:

$$\phi_e^* = \zeta_w/\phi_{\text{ref}} = 0 \text{ on the pore surface} \tag{17}$$

$$\phi_e^* = 0, \text{ as } |z^*| \to \infty, \text{ r}^* < b/a \tag{18}$$

$$\mathbf{n}\cdot\nabla^*\delta\phi^* = 0 \text{ on the pore surface} \tag{19}$$

$$\mathbf{n}\cdot\nabla^*\,\delta\phi^* = -E^*, \text{ as } |z^*| \to \infty, r^* < b/a \tag{20}$$

$$\mathbf{n}\cdot\nabla^* g_j = 0\; j = 1{,}2 \text{ on the pore surface} \tag{21}$$

$$g_j^* = -\delta\phi^*, j = 1{,}2, \text{ as } |z^*| \to \infty, r^* < b/a \tag{22}$$

$$\mathbf{u}^* = -U_p^*\mathbf{e}_z \text{ on the pore surface} \tag{23}$$

$$\mathbf{u}^* = -U_p^*\mathbf{e}_z, \text{ as } |z^*| \to \infty, r^* < b/a \tag{24}$$

Here, $E^* = E/E_{\text{ref}}$, $r^* = r/a$, and $z^* = z/a$ with $E_{\text{ref}} = \phi_{\text{ref}}/a$; ζ_w is the surface potential of the pore; I_0 is the modified Bessel function of the first kind of order zero; $\mathbf{n}$ is the unit normal vector directed into the fluid phase. In addition, we assume that the permittivity of the fluid phase inside the polyelectrolyte is the same as that outside the polyelectrolyte,[23–25] which is justified experimentally to be reasonable.[69] This implies that both the electrical potential and the electric field are continuous on the polyelectrolyte-fluid interface. Similarly, the viscosity of the fluid phase inside the polyelectrolyte is assumed to be the same as that outside the polyelectrolyte and, therefore, the fluid velocity and both its normal and tangential stresses are continuous on the polyelectrolyte-fluid interface. In summary, we assume that the following quantities are continuous on the polyelectrolyte-fluid interface: ϕ_e^*, $\delta\phi^*$, g_j^*, $\mathbf{n}\cdot\nabla^*\phi_e^*$, $\mathbf{n}\cdot\nabla^*\delta\phi^*$, $\mathbf{n}\cdot\nabla^* g_j^*$, $\mathbf{u}^*$, $\mathbf{n}\cdot\mathbf{u}^*$, $\mathbf{n}\times\mathbf{u}^*$, $\mathbf{n}\cdot(\boldsymbol{\sigma}^{\mathbf{H}^*}\cdot\mathbf{n})$, and $\mathbf{n}\times(\boldsymbol{\sigma}^{\mathbf{H}^*}\cdot\mathbf{n})$. Here, $\boldsymbol{\sigma}^{\mathbf{H}^*} = \boldsymbol{\sigma}^{\mathbf{H}}/[\varepsilon(\phi_{\text{ref}})^2/a^2]$ is the scaled hydrodynamic stress tensor with $\boldsymbol{\sigma}^{\mathbf{H}} = -\delta_P\mathbf{I} + 2\eta\boldsymbol{\Delta}$ being the hydrodynamic stress tensor, and $\mathbf{I}$, $\boldsymbol{\Delta} = [\nabla\mathbf{u} + (\nabla\mathbf{u})^{\mathbf{T}}]/2$, and the superscript $\mathbf{T}$ being the unit tensor, the rate of deformation tensor, and matrix transpose, respectively. The nature of the geometry considered also requires that ϕ_e^*, $\delta\phi^*$, g_j^*, $\mathbf{u}^*$, and $\delta_P{}^*$ are all symmetric about $r^* = 0$.

Note that because the particle velocity is unknown, the boundary conditions such as eqn (23) and (24) cannot be applied directly and, therefore, solving the present problem involves a tedious trial-and-error procedure. This difficulty can be avoided by adopting the solution strategy proposed by O'Brien and White,[6] which has also been applied in the analyses of other similar problems.[16,17,46] The rationale behind this approach is that both the governing equations and the associated boundary conditions are linear with respect to the strength of the applied electric field. Therefore, both of them can be partitioned mathematically into two sub-problems. In sub-problem one, the pore and the bulk fluid move at a constant relative velocity $-U_p$ without applying $\mathbf{E}$, and in sub-problem two $\mathbf{E}$ is applied but the pore and the bulk fluid are stagnant. If we let $\mathbf{F_i}$ be the total force acting on the polyelectrolyte in the z-direction in sub-problem i and F_i be its magnitude, then $F_1^* = f_1 U_p^*$ and $F_2^* = f_2 E^*$ with $F_i^* = F_i/\varepsilon(\phi_{\text{ref}})^2$ being the corresponding scaled forces. The proportional constants f_1 and f_2 are independent of U_p^* and E^*, respectively. At steady state ($F_1^* + F_2^* = 0$) must vanish, yielding[21,46]

$$\mu^* = \frac{U_p^*}{E^*} = -\frac{f_2}{f_1} \tag{25}$$

where μ^* is the scaled electrophoretic mobility of the polyelectrolyte. In our case, the forces acting on the polyelectrolyte include the electrical force $\mathbf{F_e}$ and the hydrodynamic force $\mathbf{F_h}$, and only the z-components of these forces need be considered. Therefore, if we let F_{ei} and F_{hi} be the z-components of $\mathbf{F_e}$ and $\mathbf{F_h}$ in sub-problem i, respectively, and $F_{ei}^* = F_{ei}/\varepsilon(\phi_{\text{ref}})^2$ and $F_{hi}^* = F_{hi}/\varepsilon(\phi_{\text{ref}})^2$ be the corresponding scaled quantities, then $F_i^* = F_{ei}^* + F_{hi}^*$, $i = 1{,}2$. F_{ei}^*[63,70] and F_{hi}^*[61,63,71,72] can be evaluated by

$$\begin{aligned} F_{ei}^* &= \iint_{S^*} (\boldsymbol{\sigma}^{\mathbf{E}^*}\cdot\mathbf{n})\cdot\mathbf{e}_z dS^* \\ &= \iint_{S^*} \left(\left[\frac{\partial\phi_e^*}{\partial n}\frac{\partial\delta\phi^*}{\partial z^*} + \frac{\partial\delta\phi^*}{\partial n}\frac{\partial\phi_e^*}{\partial z^*} \right] - \left[\frac{\partial\phi_e^*}{\partial n}\frac{\partial\delta\phi^*}{\partial n} \right. \right. \\ &\quad \left. \left. + \frac{\partial\phi_e^*}{\partial t}\frac{\partial\delta\phi^*}{\partial t} \right] n_z \right) dS^* \end{aligned} \tag{26}$$

$$F_{hi}^* = \iint_{S^*} (\boldsymbol{\sigma}^{\mathbf{H}^*}\cdot\mathbf{n})\cdot\mathbf{e}_z dS^* \tag{27}$$

Here, $\boldsymbol{\sigma}^{\mathbf{E}^*} = \boldsymbol{\sigma}^{\mathbf{E}}/[\varepsilon(\phi_{\text{ref}})^2/a^2]$ is the scaled Maxwell stress tensor with $\boldsymbol{\sigma}^{\mathbf{E}} = \varepsilon\mathbf{EE} - (1/2)\varepsilon E^2\mathbf{I}$ being the Maxwell stress tensor and $E^2 = \mathbf{E}\cdot\mathbf{E}$; $S^* = S/a^2$ is the scaled surface area with S being the polyelectrolyte surface; n_z, n, and t are the z-component of the unit normal vector $\mathbf{n}$, the magnitude of $\mathbf{n}$, and the magnitude of the unit tangential vector $\mathbf{t}$, respectively.

Note that in sub-problem one, $U_p^* \neq 0$ and $E^* = 0$, and in sub-problem two, $U_p^* = 0$ and $E^* \neq 0$. For a given E^*, the solution procedure includes the following steps.[64] (i) Assume an arbitrary value for U_p^* and solve eqn (9)–(14) subject to eqn (17)–(24). (ii) Calculate F_{ei}^* and F_{hi}^* by eqn (26) and (27), respectively, and evaluate $F_i^* = F_{ei}^* + F_{hi}^*$, $i = 1{,}2$. (iii) Use $F_1^* = f_1 U_p^*$ and $F_2^* = f_2 E^*$ to calculate f_1 and f_2. (iv) Apply eqn (25) to evaluate μ^*. Note that if we let $U_p^* = E^*$, then μ^* can also be evaluated directly by $-(F_2^*/F_1^*)$.

For convenience, the rescaled electrophoretic mobility defined below is used in subsequent discussion:

$$\mu_s^* = \frac{\mu^*}{Q_{fix}/(\lambda a)^2} \quad (28)$$

Note that if the electrolyte concentration is very high ($\kappa a \to \infty$), eqn (2) gives $\mu \to \rho_{fix}/\eta\lambda^2$ and, therefore, $\mu^* \cong \mu/(U_{ref}/E_{ref}) = (\rho_{fix}/\eta\lambda^2)(\eta/\varepsilon\phi_{ref}) = Q_{fix}/(\lambda a)^2$, yielding $\mu_s^* \to 1$. Here, $\mu^* \cong Q_{fix}/(\lambda a)^2$ is the scaled electrophoretic mobility of an individual polymer segment or monomer.[73] In other words, the mobility of a spherical polyelectrolyte at a very high electrolyte concentration is essentially that of one resistance center, that is, the polyelectrolyte becomes freely drained and there is no hydrodynamic interaction between its resistance centers.[28,61]

3. Results and discussion

FlexPDE (PDE Solutions, Spokane Valley, WA) is adopted to solve the present problem numerically. Grid independence is checked during the solution procedure to ensure that the mesh used is appropriate. Typically, using a total of *ca.* 9,500 and 3,200 nodes is sufficient for obtaining reasonably accurate results for the electric field and the flow field, respectively. The end effect of the cylindrical pore can be neglected if its length exceeds *ca.* 12 times of the particle radius.[46,50] The applicability of the software adopted is first justified by applying it to the case of an isolated, positively charged porous sphere in an infinite electrolyte medium, which was solved analytically by Hermans and Fujita.[32] Because the effect of DLP is neglected in their analysis, a small value is assumed for Q_{fix}. Fig. 2 shows the variations of the rescaled electrophoretic mobility μ_s^* as a function of κa at various values of Λ ($= a/b$) for a positively charged spherical polyelectrolyte in an uncharged cylindrical pore. Note that if Λ is sufficiently small and κa is sufficiently large, then the presence of the pore can be neglected and, therefore, the present result should reduce to that of Hermans and Fujita.[32] As can be seen in Fig. 2, this is indeed the case, implying that the performance of the numerical scheme adopted is satisfactory.

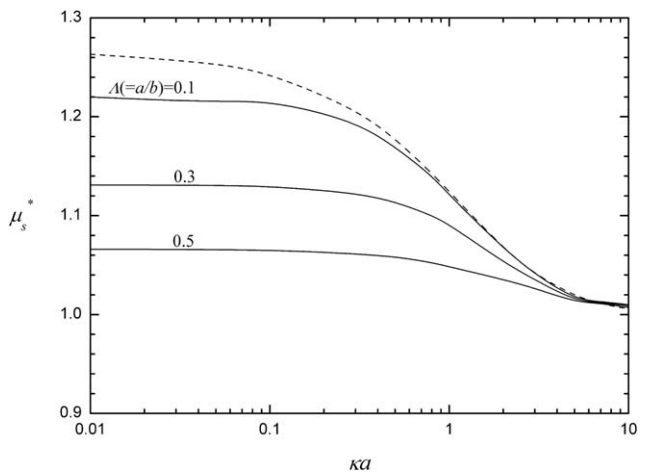

Fig. 2 Variation of the rescaled electrophoretic mobility μ_s^* as a function of κa at various values of Λ ($= a/b$) for the electrophoresis of a positively charged spherical polyelectrolyte along the axis of an uncharged cylindrical pore at $\zeta_w = 0$, $Q_{fix} = 1$, $\lambda a = 1$, and $Pe_1 = Pe_2 = 0.1$. Solid curves: present numerical results; dashed curve: analytical result for an isolated porous sphere.[32]

In the subsequent discussion, the influences on the electrophoretic behavior of the parameters key to the present problem, including the thickness of double layer, the relative size of the pore, and the nature of the polyelectrolyte are examined. Typically, the linear size of polyelectrolytes ranges from 10^{-3} to 10 μm, that of a pore from 10^{-2} to 100 μm, and λ^{-1} ranges from 0.1 to 10 nm.[27,66–68,74] These provide a rough estimate for the ranges of the parameters used in the numerical simulation. In addition, we assume that $z_1 = -z_2$, that is, $\alpha = 1$, and $Pe_1 = Pe_2 = 0.1$,[46,64] for illustration.

3.1 Influence of double layer thickness κa

The influence of the thickness of double layer, measured by parameter κa, on the rescaled electrophoretic mobility of the polyelectrolyte μ_s^* at various values of Q_{fix} is illustrated in Fig. 3. The corresponding rescaled electric force $F_{e2,s}^*$ ($= F_{e2}^*/[Q_{fix}/(\lambda a)^2]$), rescaled hydrodynamic force $F_{h2,s}^*$ ($= F_{h2}^*/[Q_{fix}/(\lambda a)^2]$), and the net rescaled driving force $F_{2,s}^*$ ($= F_2^*/[Q_{fix}/(\lambda a)^2]$) acting on the polyelectrolyte in the z-direction in the second sub-problem are also presented. Here, $F_s^* = F^*/[Q_{fix}/(\lambda a)^2]$ with $F^* = F/\varepsilon(\phi_{ref})^2$. For convenience, we fix the radius of the polyelectrolyte a and, therefore, κa varies implying that the bulk electrolyte

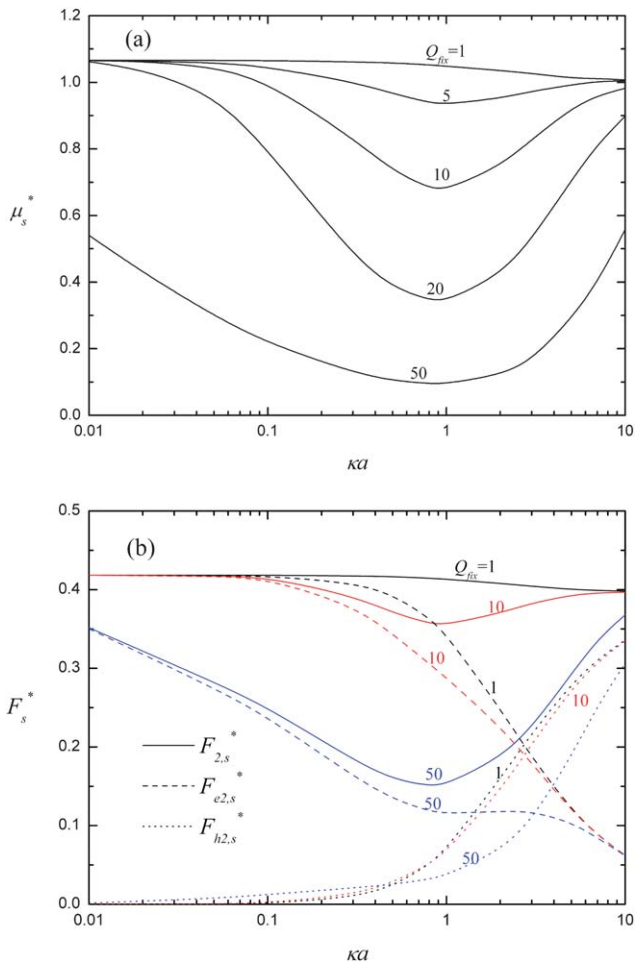

Fig. 3 Variations of the rescaled electrophoretic mobility μ_s^*, (a), and the corresponding rescaled forces in sub-problem two, $F_{e2,s}^*$, $F_{h2,s}^*$, and $F_{2,s}^*$, (b), as a function of κa at various values of Q_{fix} at $\Lambda = 0.5$, and $\lambda a = 1$.

concentration varies. Fig. 3(a) reveals that if Q_{fix} is small (= 1), μ_s^* decreases monotonically with increasing κa, and if κa is sufficiently large, then $\mu_s^* \to 1$. The later results from the fact that, as mentioned previously, μ^* must approach the scaled electrophoretic mobility of an individual polymer segment or monomer as $\kappa a \to \infty$.[73] The result that μ_s^* decreases with increasing κa is also observed in the cases of biological cells[69,75,76] and synthetic polyelectrolytes,[77] but the opposite trend is observed in the cases of rigid particles having constant surface potential[3,6] or constant surface charge density[48] and soft particles.[16,20–22] In the present case, the decrease in μ_s^* with increasing κa can be explained as follows: the larger the κa (thinner double layer) the larger the amount of counterions that is confined to the interior of the polyelectrolyte, yielding a smaller electrical driving force acting on the polyelectrolyte, as is justified in Fig. 3(b). As shown in Fig. 3(a), the behavior of μ_s^* at large Q_{fix} is qualitatively different from that at small Q_{fix}. In the former, μ_s^* goes through a local minimum before it approaches unity as κa increases. The presence of a local minimum in the mobility as κa varies is also observed in the theoretical study of O'Brien and White[6] for a rigid sphere in an infinite fluid, that of He and Lee[38] for a concentrated dispersions of charged porous spheres, and in several experimental studies for porous particles.[78–80] As justified by Fig. 3(b), the behaviors of μ_s^* seen in Fig. 3(a) can be explained by the competition of the shielding effect,[36] the effect of DLP,[6,21,38,46] and the electroosmotic retardation flow.[16,17,46,50] As will be justified later in the discussion of the distribution of the ionic species, the shielding effect comes from the fixed charges inside the polyelectrolyte attracting counterions which flow in and repulsing coions which flow out. The inflow of the counterions in the presence of the applied electric field depresses the local electric field near the polyelectrolyte surface appreciably.[36] The effect of DLP arising from the convective motion of ionic species induces an internal electric field, which has the direction opposite to that of the applied electric field, thereby reducing the mobility of the polyelectrolyte,[6,21,38,46] as will be illustrated later. In addition, as will be justified later, the larger the Q_{fix} the more significant the shielding effect and the effect of DLP, both have the effect of reducing the electrical driving force. The electroosmotic retardation flow, which has an important influence on the drag force acting on a particle comes from the unbalanced amount of counterions in the double layer surrounding the particle when an external electric field is applied.[22,46,50] In the present case, it is a counterclockwise (clockwise) recirculation flow on the right-hand (left-hand) side of the polyelectrolyte, as will be illustrated later. Fig. 3(b) shows that $F_{e2,s}^*$ decreases with increasing κa, which is due to the presence of the effect of DLP and the decrease in the effective charge density, $(\rho + \rho_{fix})$, inside the polyelectrolyte as κa increases. The later is because the larger the κa the thinner the double layer and the greater the amount of counterions confined in the interior of the polyelectrolyte, yielding a smaller electrical driving force coming from the effective fixed charge. The former is important when κa is on the order of unity, and becomes unimportant if κa is either sufficiently large or sufficiently small.[6,21,38] It is interesting to note in Fig. 3(b) that if κa is sufficiently large, then $F_{e2,s}^*$ is linearly dependent on κa, and that relationship is independent of Q_{fix}. This can be explained by the fact that if κa is sufficiently large, then the effect of DLP is unimportant, so is the shielding effect because the double layer is thin. Because the hydrodynamic stress tensor comprises a pressure component and a viscous component, $F_{hi,s}^*$ can be rewritten as[63,71]

$$F_{hi,s}{}^* = \frac{F_{hi}{}^*}{Q_{fix}/(\lambda a)^2} = F_{hi(v),s}{}^* + F_{hi(p),s}{}^* \tag{29}$$

where

$$F_{hi(v),s}{}^* = \frac{\iint_S \left[t_z \eta \left(\frac{\partial u_n}{\partial t} + \partial \frac{u_t}{\partial n} \right) + n_z \left(2\eta \frac{\partial u_n}{\partial n} \right) \right] dS \Big/ \varepsilon \left(\phi_{ref} \right)^2}{Q_{fix}/(\lambda a)^2} \tag{30}$$

$$F_{hi(p),s}{}^* = \frac{\iint_S (-\delta p n_z) dS \Big/ \varepsilon \left(\phi_{ref} \right)^2}{Q_{fix} \Big/ (\lambda a)^2} \tag{31}$$

In these expressions, $F_{hi(v),s}^*$ and $F_{hi(p),s}^*$ are the rescaled viscous component and the rescaled pressure component of the rescaled hydrodynamic force, respectively; $u_n = \mathbf{u} \cdot \mathbf{n}$ and $u_t = \mathbf{u} \cdot \mathbf{t}$; t_z is the z-component of the unit tangential vector $\mathbf{t}$. As seen in Fig. 3(b), $F_{h2,s}^* > 0$, and increases with increasing κa. The former is because the positive pressure term dominates. The latter is because the larger the κa (the thinner the double layer) the less significant the shielding effect suppressing the double layer is and, therefore, the greater the amount of counterions (coions) condensed inside (outside) the polyelectrolyte. This makes the counterclockwise electroosmotic retardation flow around the polyelectrolyte more significant, and therefore, a greater $F_{h2(v),s}^*$. The qualitative behavior of $F_{2,s}^*$ in Fig. 3(b) is similar to that of μ_s^* in Fig. 3(a), namely, if Q_{fix} is small (= 1), $F_{2,s}^*$ decreases with increasing κa, and if Q_{fix} is large, then $F_{2,s}^*$ exhibits a local minimum. This is because if Q_{fix} is small, $F_{2,s}^*$ is dominated by $F_{e2,s}^*$, but if Q_{fix} is large, $F_{2,s}^*$ is dominated by $F_{e2,s}^*$ when κa is small and by $F_{h2,s}^*$ when κa is large. If Q_{fix} is small, because the electrical potential of the system under consideration is low, both the shielding effect and the effect of DLP are insignificant and, therefore, the rate of decrease in $F_{e2,s}^*$ as κa increases is always faster than the rate of increase in $F_{h2,s}^*$. On the other hand, if Q_{fix} is large, because both the shielding effect and the effect of DLP become significant, the rate of decrease in $F_{e2,s}^*$ as κa increases is faster than the rate of increase in $F_{h2,s}^*$ when κa is small, and that trend is reversed when κa is large. We conclude that, except for the case of very thin double layer, both the shielding effect and the effect of DLP have a significant influence on the electrophoretic behavior of the polyelectrolyte. Moreover, the larger the Q_{fix}, the more significant these effects are, yielding the presence of the local minimum in μ_s^*. Fig. 3(a) suggests that if κa is sufficiently small, then μ_s^* becomes independent of Q_{fix}, implying that μ^* increases linearly with Q_{fix}, except when Q_{fix} is large. As will be explained later, this is because if Q_{fix} is large, counterion condensation occurs.

3.2 Shielding effect and counterion condensation

Fig. 4 illustrates the distribution of the number concentration of ionic species j, n_j, $j = 1, 2$, on the half plane $\theta = 0$ in the case of Fig. 3. Due to electrical interaction, counterions (anions) are

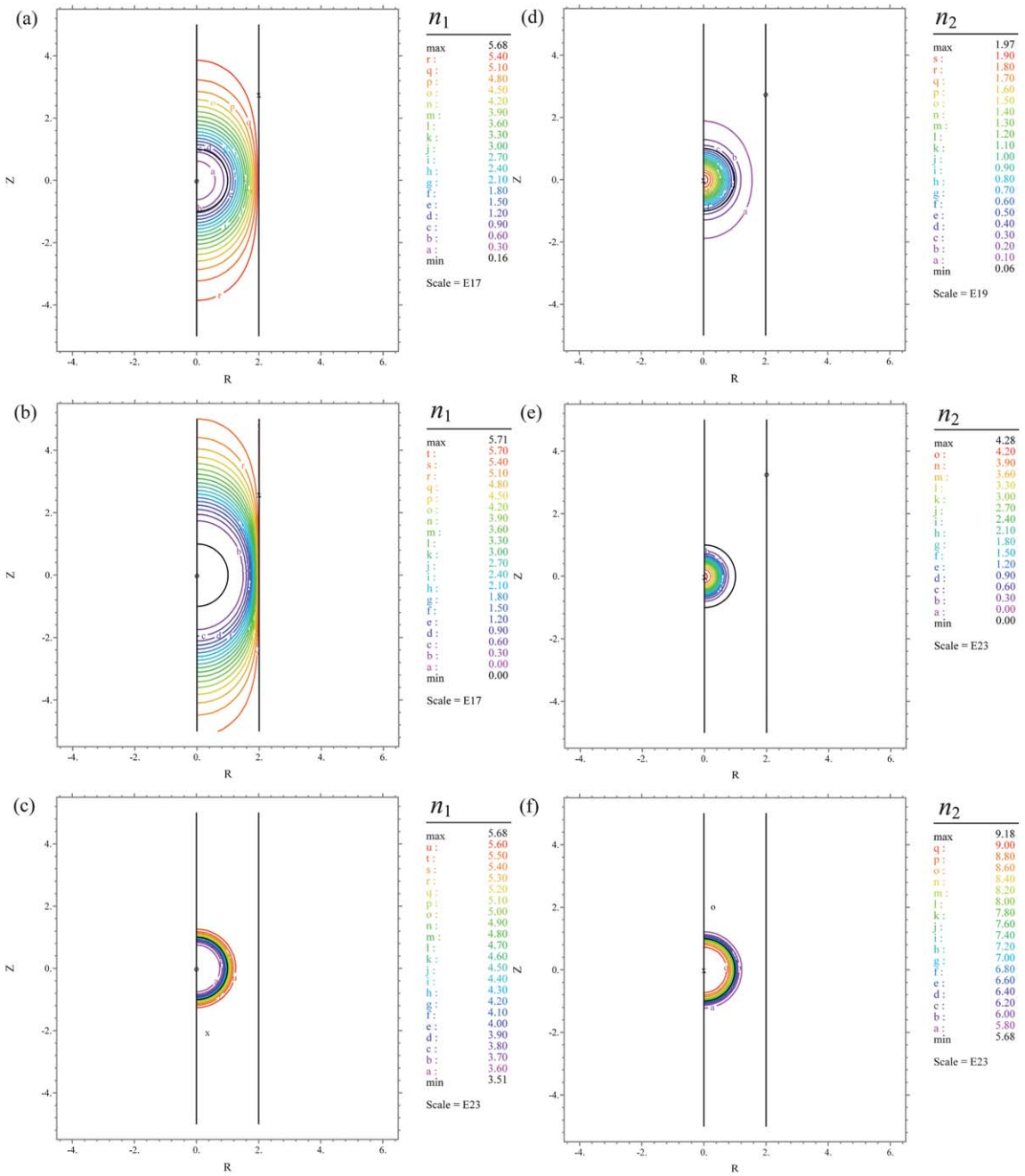

Fig. 4 Contours of the number concentration n_j on the half plane $\theta = 0$, at various combinations of Q_{fix} and κa in the case of Fig. 3, where $Z = z/a = z^*$ and $R = r/a$. (a) $j = 1$, $Q_{fix} = 10$, $\kappa a = 0.01$; (b) $j = 1$, $Q_{fix} = 50$, $\kappa a = 0.01$; (c) $j = 1$, $Q_{fix} = 50$, $\kappa a = 10$; (d) $j = 2$, $Q_{fix} = 10$, $\kappa a = 0.01$; (e) $j = 2$, $Q_{fix} = 50$, $\kappa a = 0.01$; (f) $j = 2$, $Q_{fix} = 50$, $\kappa a = 10$.

attracted into the polyelectrolyte and coions (cations) are repelled from the polyelectrolyte; the larger Q_{fix} the more significant this phenomenon is. As Q_{fix} reaches a critical value, the net charge inside the polyelectrolyte drops suddenly to a low value, known as counterion condensation.[54,55] As illustrated in Fig. 4(b) and 4(e), where counterion condensation occurs, coions are repelled from the polyelectrolyte, reflected by a small n_1 inside and immediately outside the polyelectrolyte, and counterions are attracted to deep inside the polyelectrolyte, reflected by a large n_2 near its center. It is interesting to see that in Fig. 4(c) and 4(f) as κa gets larger (double layer is thin), because the shielding effect (or counterion condensation) coming from Q_{fix}, which suppresses the double layer, becomes relatively insignificant, and therefore, coions (counterions) gathered near the outer (inter) polyelectrolyte surface. This mechanism was conjectured previously,[38] and is now justified. The distribution of the coins and counterions near the polyelectrolyte surface enhances the counterclockwise electroosmotic retardation flow near the polyelectrolyte-fluid interface, as mentioned previously. The influence of the shielding effect and the effect of counterion

condensation on the electrophoretic behavior of the polyelectrolyte will be discussed in detail later.

3.3 Double-layer polarization

If the surface potential is sufficiently high, then the effect of DLP, the deformation of ionic cloud surrounding the particle due to the convective motion of the ionic species inside double layer, needs be considered. In this case, using the original non-linear Poisson–Boltzmann equation, eqn (9), is necessary. To measure the increase in the amount of mobile ions arising from the application of **E**, we define the net perturbed ionic concentration difference, PCD, as $PCD = (\delta n_1 - \delta n_2) = [(n_1 - n_{1e}) - (n_2 - n_{2e})]$, where δn_j and n_{je}, $j = 1,2$, are the perturbed and the equilibrium number concentrations of ionic species j, respectively. As seen in Fig. 5, if the polyelectrolyte is positively charged, $PCD > 0$ in the upper region between the polyelectrolyte and the pore, and $PCD < 0$ in the lower region between the polyelectrolyte and the pore. This implies that the number of counterions (anions) increased due to the application of **E** being larger than that of the coions (cations) in the bottom region of the polyelectrolyte than that in its top region. That is, the application of **E** yields an internal electric field, which has the opposite direction to that of **E**, and therefore, the mobility of the polyelectrolyte is reduced. This phenomenon is called the effect of DLP. As can be seen in Fig. 5, the larger the Q_{fix} the more significant that effect is. In addition, if Q_{fix} is fixed, then the effect of DLP becomes unimportant when κa is either sufficiently small (thick double layer) or sufficiently large (thin double layer).

3.4 Electroosmotic retardation flow

Fig. 6 shows the typical flow field for the case of a positively charged polyelectrolyte in sub-problem two, where **E** is applied but the pore and the bulk fluid are stagnant. As seen in this figure, the fluid flows from the top region of the polyelectrolyte to its bottom region along the axis of the pore, and the scaled velocity in the bottom region of the polyelectrolyte is larger than that in its top region. Note that a counterclockwise (clockwise) flow field is present near the right- (left-) hand side of the polyelectrolyte. This is the electroosmotic retardation flow mentioned previously; the larger the κa the more significant it is. In the present case, because the rate of the strain is positive across the surface of the polyelectrolyte $F^*_{h2(v),s}$ is positive. If this phenomenon becomes significant, the electrophoretic behavior of the polyelectrolyte is dominated by the electroosmotic retardation flow, as is seen in Fig. 3(a) for the case where both κa and Q_{fix} are large. It is interesting to note that the fluid velocity flowing inside the polyelectrolyte is faster than that outside the polyelectrolyte, that is, the fluid velocity is accelerated as it flows into the polyelectrolyte. It can be inferred from eqn (11) and (12) that the electroosmotic retardation flow is accelerated by the equilibrium

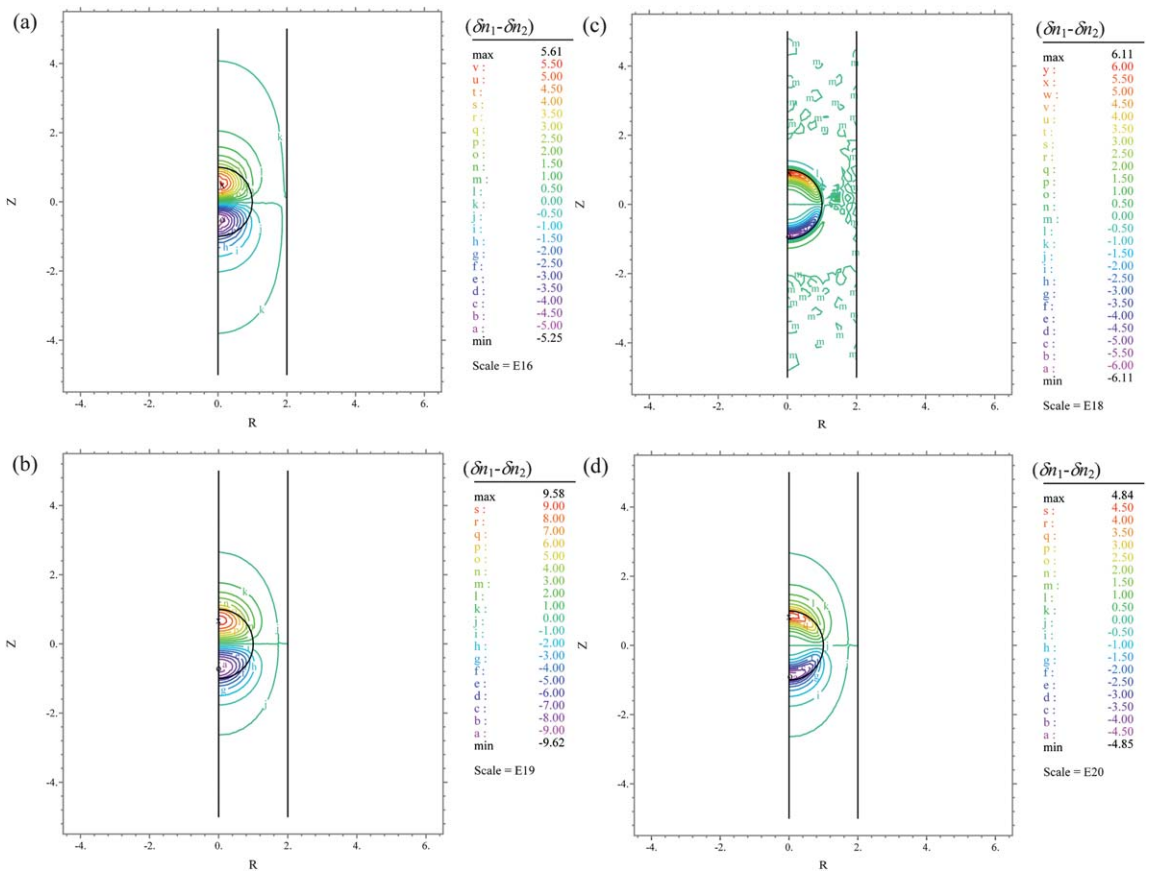

Fig. 5 Contours of the net perturbed ionic concentration difference ($\delta n_1 - \delta n_2$) in sub-problem two on the half plane $\theta = 0$ at various combinations of Q_{fix} and κa for the case of Fig. 3. (a) $Q_{fix} = 10$ and $\kappa a = 0.01$; (b) $Q_{fix} = 10$ and $\kappa a = 1$; (c) $Q_{fix} = 10$ and $\kappa a = 10$; (d) $Q_{fix} = 50$ and $\kappa a = 1$.

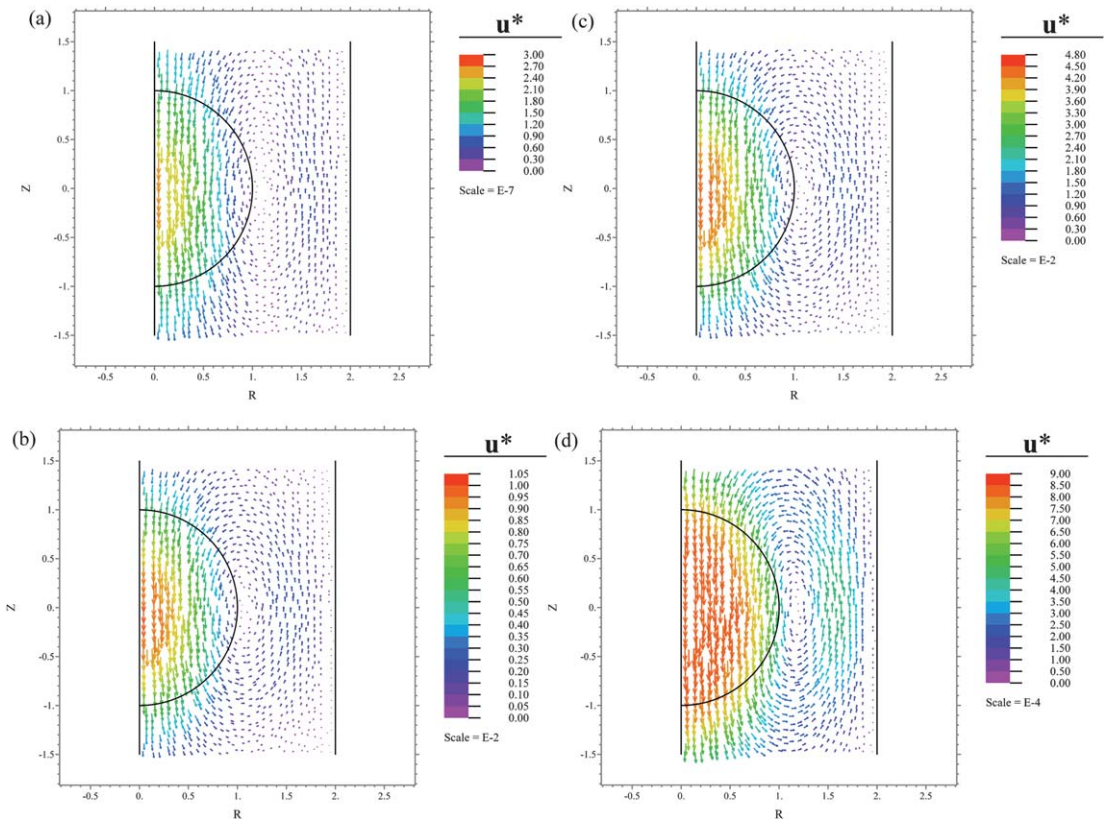

Fig. 6 Contours of the scaled velocity, $\mathbf{u}^*$, in sub-problem two on the half plane $\theta = 0$ for various combinations of κa and λa at $\Lambda = 0.5$. (a) $Q_{fix} = 10$, $\kappa a = 0.01$, and $\lambda a = 1$; (b) $Q_{fix} = 10$, $\kappa a = 10$, and $\lambda a = 1$; (c) $Q_{fix} = 50$, $\kappa a = 10$, and $\lambda a = 1$; (d) $Q_{fix} = 10$, $\kappa a = 10$, and $\lambda a = 10$.

electric field inside the polyelectrolyte. Note that the closer to the center of the polyelectrolyte the stronger electric field is, and therefore, the faster the electroosmotic retardation flow. Fig. 6 also indicates that the larger the λa the less significant the electroosmotic retardation flow, which is expected because the lager the λa the more compact the polyelectrolyte structure and, therefore, the harder for the fluid to penetrate, making the electroosmotic retardation flow less significant.

3.5 Influence of scaled friction coefficient λa

The influence of the scaled friction coefficient of a polyelectrolyte, measured by λa, on its rescaled electrophoretic mobility μ_s^* is illustrated in Fig. 7(a). It is interesting to note that the behavior of μ_s^* depends highly upon the levels of λa: if λa is small, μ_s^* has a local minimum as κa varies; if λa is large, μ_s^* decreases with increasing κa. Again, this arises from the competition of the shielding effect, the effect of DLP, and the electroosmotic retardation flow. The presence of the local minimum in μ_s^* can be explained by the same reasoning as that employed in the discussion of Fig. 3. The monotonic decrease in μ_s^* with increasing κa can be explained by the variations of the rescaled forces acting on the polyelectrolyte in the second sub-problem, $F_{e2,s}^*$, $F_{h2,s}^*$, and $F_{2,s}^*$, illustrated in Fig. 7(b). If λa is large, the trend of μ_s^* is similar to that of $F_{2,s}^*$, which is dominated by $F_{e2,s}^*$. This is because if λa is large, then the electroosmotic retardation flow becomes unimportant, so is $F_{h2,s}^*$, as is observed in Fig. 6(d). In this case, the larger the κa, the thinner the double layer and the larger the amount of counterions gathered in the interior of the polyelectrolyte, yielding a smaller electrical driving force acting on the polyelectrolyte. Note that μ_s^* must approach unity as $\kappa a \to \infty$.[38,73] The disappearance of the local minimum in μ_s^* as κa varies under the conditions of large Q_{fix} and λa has not been found previously for soft particles. Therefore, we conclude that the friction coefficient of a polyelectrolyte plays a key role in the description of its electrophoretic behavior, both quantitatively and qualitatively.

3.6 Influence of counterion condensation

Let us discuss further on the effect of counterion condensation by examining the variation of the scaled electrophoretic mobility of the polyelectrolyte μ^* as a function of Q_{fix} at various combinations of κa and Λ ($= a/b$) presented in Fig. 8. As seen in this figure, if Q_{fix} is small, μ^* increases roughly linearly with Q_{fix} except for the case of $\kappa a = 1$, and if Q_{fix} is large, then μ^* has a local maximum as Q_{fix} varies. These results are similar to those observed in the electrophoresis of a spherical dispersion of rigid particles in a salt-free solution.[81] The approximate linear dependence of μ^* on Q_{fix} can be explained by the fact that if Q_{fix} is small, the effect of DLP is unimportant except when the Debye length is of the order of the radius of the polyelectrolyte (*i.e.*, $\kappa a \cong 1$), as illustrated in Fig. 5. It can be inferred that, if Q_{fix} is large, then the effect of DLP is significant, yielding an nonlinear relationship between μ^* and Q_{fix}. The presence of the local maximum in μ^* has not been found in previous theoretical studies

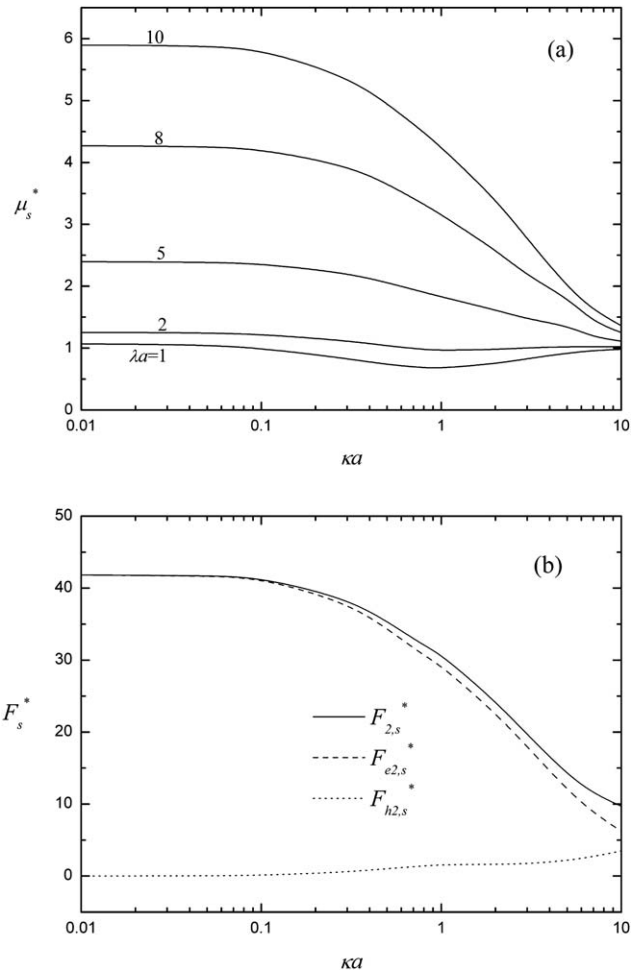

Fig. 7 Variations of the rescaled electrophoretic mobility μ_s^*, (a), and the rescaled forces in sub-problem two, $F_{e2,s}^*$, $F_{h2,s}^*$, and $F_{2,s}^*$, at $\lambda a = 10$ for the case of (a), (b), as a function of κa at various of λa at $Q_{fix} = 10$ and $\Lambda = 0.5$.

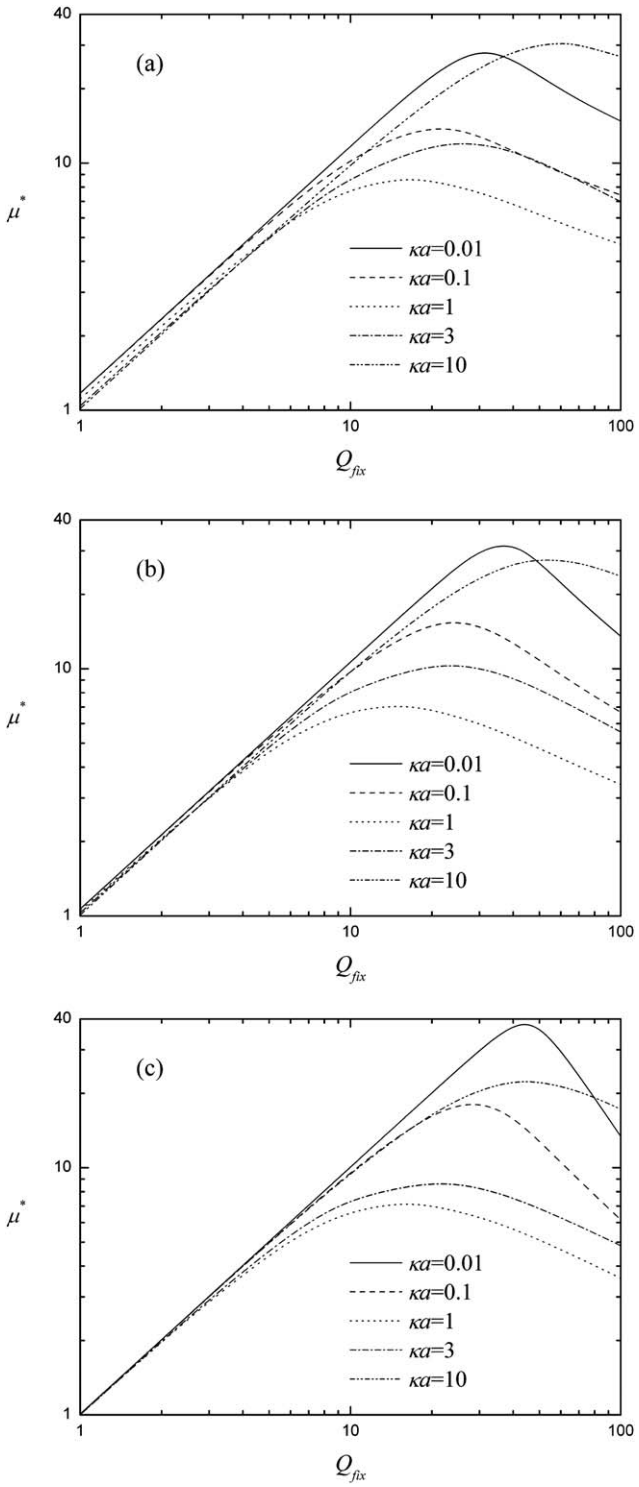

Fig. 8 Variation of the scaled electrophoretic mobility μ^* as a function of Q_{fix} at various combinations of κa and Λ at $\lambda a = 1$. (a) $\Lambda = 0.2$, (b) $\Lambda = 0.5$, (c) $\Lambda = 0.8$.

where the effect of DLP is neglected. Some experimental studies,[56,57] however, reveal the possible presence of a local maximum in μ^*. The experimental observations that the mobility of a particle becomes independent of the amount of charge placed on a polymer of fixed length once a critical charge loading is reached,[56,57] and that mobility shows a discontinuity as the scaled linear charge density parameter, $\xi = e^2/4\pi\varepsilon k_B T\bar{b}$ with $\bar{b}$ being the axial spacing between neighboring bound charge groups, varies[56–58] may both be caused by the effect of counterion condensation. It can be inferred that the presence of this effect arises mainly from the fact that counterion condensation makes the effective charge density in the polyelectrolyte (ρ_{fix} + ρ) and, therefore, the electrical driving force, decreases appreciably. Note that the effect of DLP, which reduces the electrical driving force, can also play a role. However, if double layer is very thin, then both the effects of counterion condensation and DLP become unimportant, and μ^* is dominated by the electroosmotic retardation flow. This suggests that the rationale behind the presence of the local maximum in μ^* seen in Fig. 8 at different thickness of double layer is also different. For convenience, we define the critical value of Q_{fix}, $Q_{fix,c}$, at which μ^* has the local maximum μ_c^*. As can be explained by the variations of the scaled net driving forces F_1^* and F_2^* shown in Fig. 9, the occurrence of the local maximum in μ^* seen in Fig. 8 comes from the competition of the counterion condensation, DLP, and electroosmotic retardation flow. Recall that in sub-problem one, the pore and the bulk

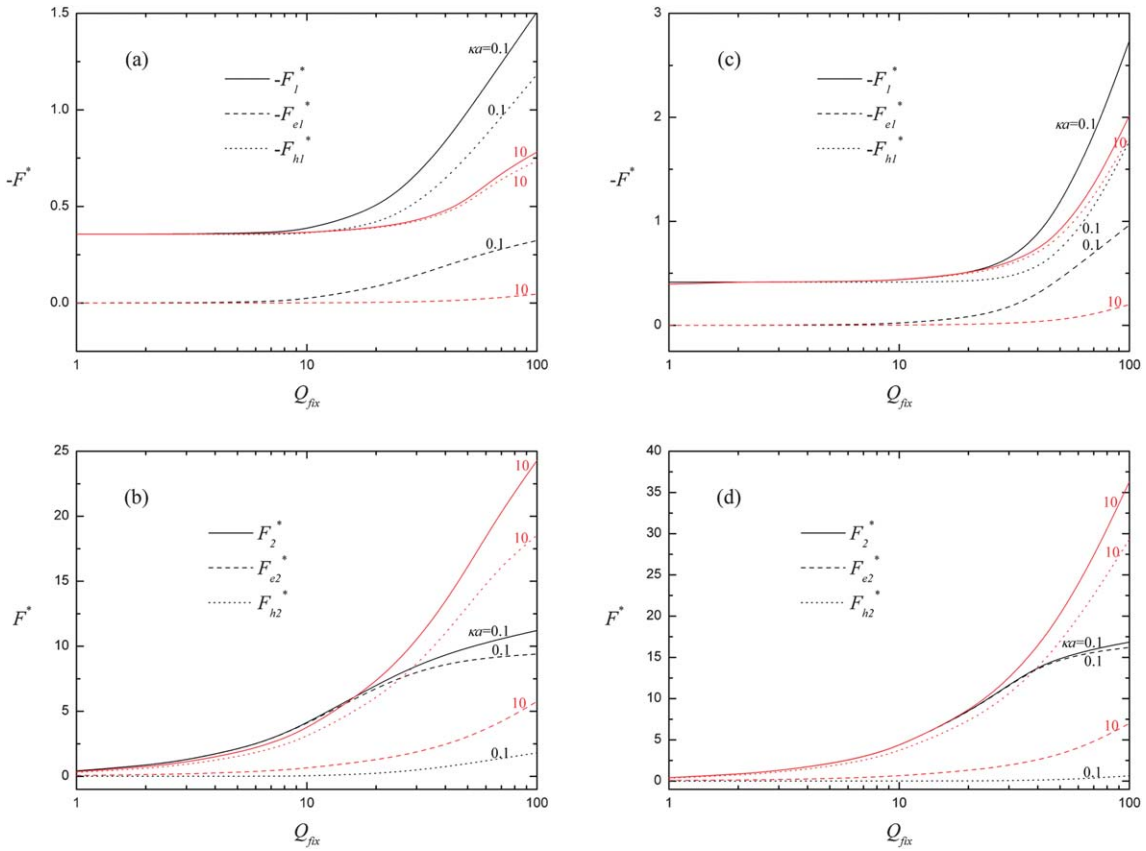

Fig. 9 Variation of the scaled forces $-F_{e1}^*$, $-F_{h1}^*$, and $-F_1^*$, (a) and (c), and F_{e2}^*, F_{h2}^*, and F_2^*, (b) and (d), as a function of Q_{fix} at various combinations of κa and Λ at $\lambda a = 1$ for the cases of Fig. 8(a), (a) and (b), and Fig. 8(c), (c) and (d).

fluid move with a relative constant velocity $-U_p^*$ in the absence of **E**. According to eqn (10)–(12), if the polyelectrolyte is in a moving electrolyte fluid, then a relaxation electric field is induced, the direction of which is the same as that of the flow of the electrolyte fluid. Therefore, the fluid surrounding the polyelectrolyte is accelerated and both the electrical force and the hydrodynamic force acting on the polyelectrolyte are raised. Fig. 10 illustrates the typical contours of the scaled net perturbed ionic concentration difference, $(\delta n_1^* - \delta n_2^*)$, in sub-problem one, and Fig. 11 shows the associated flow fields. As seen in these figures, the larger the Q_{fix} the stronger the relaxation electric field, and the faster the fluid velocity surrounding the polyelectrolyte. Note that because the present problem focused mainly on the effects of the applied electric field (sub-problem two) and the particle velocity (sub-problem one) on the electrophoretic behavior of the particle, a superposition of the flow fields of these two sub-problems is unable to provide useful information and, therefore, unnecessary. Therefore, as seen in Fig. 9(a) and 9(c), the absolute values of the scaled electric force, the scaled hydrodynamic force, and the scaled total driving force acting on the polyelectrolyte in the z-direction in sub-problem one, $|F_{e1}^*|$, $|F_{h1}^*|$, and $|F_1^*|$, respectively, all increase monotonically with increasing Q_{fix}. In sub-problem two **E** is applied but the pore and the bulk fluid remain fixed. In the present case, the shielding effect, the effect of DLP, and the electroosmotic retardation flow all play a role. The competition of these effects yields the behaviors of the scaled forces, F_{e2}^*, F_{h2}^*, and F_2^*, shown in Fig. 9(b) and 9(d). For example, if κa is small, F_2^* is dominated by F_{e2}^*, and if κa is sufficiently large, then F_2^* is dominated by F_{h2}^*. Fig. 9 suggests that for thick double layers (small values of κa), if $Q_{fix} > Q_{fix,c}$, because counterion condensation occurs and DLP is appreciable, the rate of increase in F_{e2}^* as Q_{fix} increases decreases, so is that in F_2^*. As Q_{fix} increases, although both F_2^* and $|F_1^*|$ increase, the rate of increase of the former is faster than that of the later for $Q_{fix} < Q_{fix,c}$, but slower for $Q_{fix} > Q_{fix,c}$, leading to the presence of the local maximum in μ^* seen in Fig. 8. On the other hand, for thin double layers (κa exceeds *ca.* 3), because the F_{h2}^* arising from electroosmotic retardation flow dominates, the rate of increase in F_2^* as Q_{fix} increases is faster than that in $|F_1^*|$ for $Q_{fix} < Q_{fix,c}$, and that trend is reversed for $Q_{fix} > Q_{fix,c}$. The later is because if Q_{fix} is sufficiently large, the effect of DLP arising from the moving of the electrolyte fluid in sub-problem one, which has the effect of raising both $|F_{e1}^*|$ and $|F_{h1}^*|$, becomes significant. Therefore, we conclude that if κa is small (thick double layer), the presence of the local maximum in μ^* as Q_{fix} varies comes from the combined effect of counterion condensation and DLP. In this case, μ^* is dominated by the electrical driving force. On the other hand, if κa is large, the presence of the local maximum in μ^* arises from the fact that the effect of DLP is pronounced when Q_{fix} is sufficiently large, and μ^* is dominated by the hydrodynamic drag force in this case. Fig. 8 also suggests that if κa is small, both $Q_{fix,c}$ and μ_c^* decreasewith increasing κa, but the reverse is true when κa is large. The former is because the effect of DLP, which reduces the electrical driving force, is most

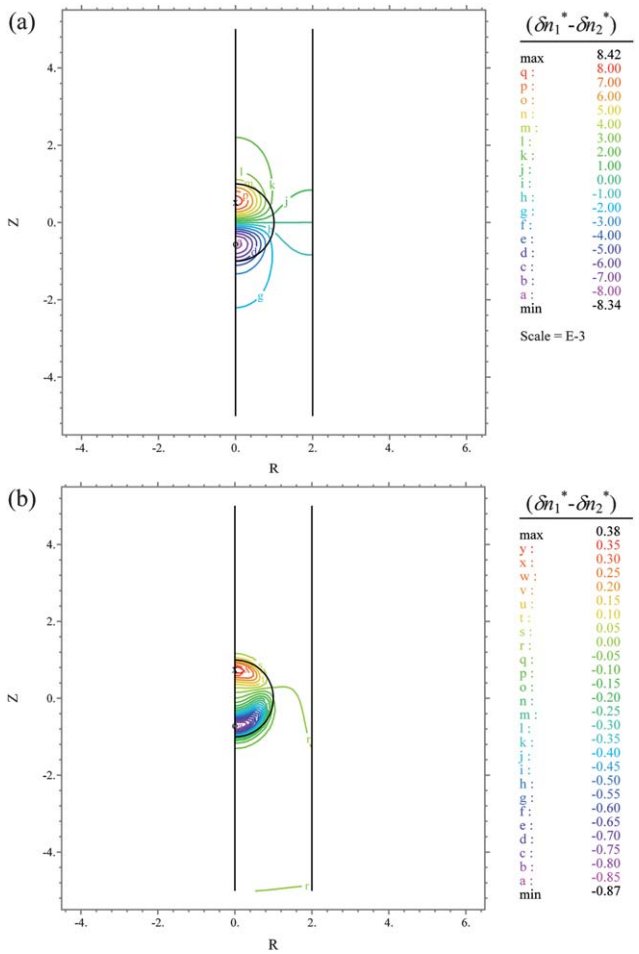

Fig. 10 Contours of the scaled net perturbed ionic concentration difference ($\delta n_1 - \delta n_2$) in sub-problem one on the half plane $\theta = 0$ for the case of $\lambda a = 1$, $\kappa a = 0.1$, and $\Lambda = 0.5$ at $Q_{fix} = 10$, (a), and $Q_{fix} = 50$, (b).

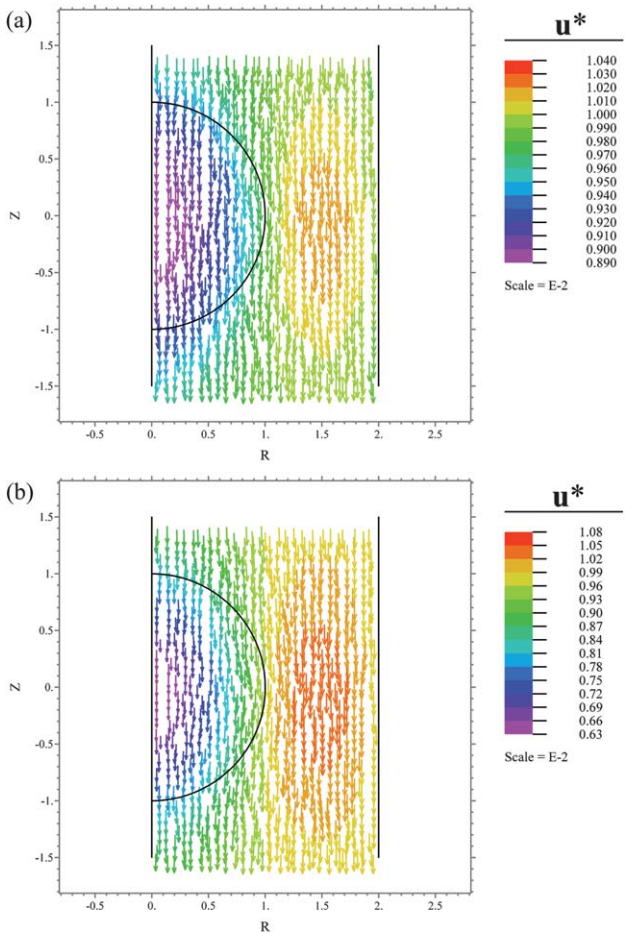

Fig. 11 Contours of the scaled velocity, $\mathbf{u}^*$, in sub-problem one on the half plane $\theta = 0$ for the case of Fig. 10. (a) $Q_{fix} = 10$; (b) $Q_{fix} = 50$.

important at $\kappa a \cong 1$, and therefore, a small value of $Q_{fix,c}$ is necessary for the occurrence of counterion condensation at that value of κa, and the corresponding μ_c^* is also small. The later is because if the double layer is thin, then both the DLP effect and the shielding effect (or counterion condensation) suppressing the double layer become unimportant, making F_2^* increases, as stated in the discussion of Fig. 3(b). Therefore, a larger value of $Q_{fix,c}$ is required to overcome these effects. Fig. 8(a)–(c) reveals that if double layer is thick ($\kappa a < 1$), then both $Q_{fix,c}$ and μ_c^* increase with increasing Λ (increasing significance of boundary effect). However, the reverse trend is observed when double layer is sufficiently thin (κaexceeds *ca.* 3). These observations can be explained by the competition of the electrical and the hydrodynamic forces acting on the polyelectrolyte. If Λ is sufficiently large, because double layer is compressed by the pore, the amount of coions compressed into the polyelectrolyte increases with increasing Λ, which has the effect of increasing F_{e2}^* (and therefore F_2^*) by alleviating both the shielding effect (or counterion condensation) and the DLP effect, as illustrated in Fig. 9(b) and 9(d). Therefore, if the electrical force dominates, then $Q_{fix,c}$ becomes large, so is μ_c^*. A larger Λ also implies a more significant boundary effect and a greater hydrodynamic retardation force, resulting in a faster rate of increase in $|F_{h1}^*|$ (and therefore $|F_1^*|$) as Q_{fix} increases, as can be seen from Fig. 9(a) and 9(c). Therefore, if the hydrodynamic force dominates, then the larger the Λ the smaller the $Q_{fix,c}$ and μ_c^*. We conclude that if κa is sufficiently large, because the effect of double layer overlapping is insignificant the behavior of μ^* is dominated by the hydrodynamic force. On the other hand, if κa is sufficiently small, then the behavior of μ^* is dominated by the electrical force.

Fig. 12(a) illustrates the variations of μ^* as a function of Q_{fix} at various combinations of λa and κa. As seen in this figure, regardless of the level of κa, if λa is small, μ^* has a local maximum; however, if λa is sufficiently large, μ^* increases monotonically with increasing Q_{fix} and approaches a plateau value. The latter implies that if λa is sufficiently large, the hydrodynamic force arising from the compacted structure of the polyelectrolyte dominates. As mentioned previously, the presence of a local maximum in μ^* is because for $Q_{fix} < Q_{fix,c}$, the rate of increase in F_2^* with increasing Q_{fix} is faster than that in $|F_1^*|$, but the reverse trend is true for $Q_{fix} > Q_{fix,c}$. The monotonic increase in μ^* with increasing Q_{fix} comes from the fact that as Q_{fix} increases, the rate of increase in F_2^* is always faster than that in $|F_1^*|$, and if Q_{fix} is sufficiently large, these two rates become the same. Fig. 12(a) also reveals that if λa is not too large, $Q_{fix,c}$ increases with increasing λa. This is because the larger the λa the more compact the polyelectrolyte structure and, therefore, the slower the fluid velocity inside, yielding a less significant

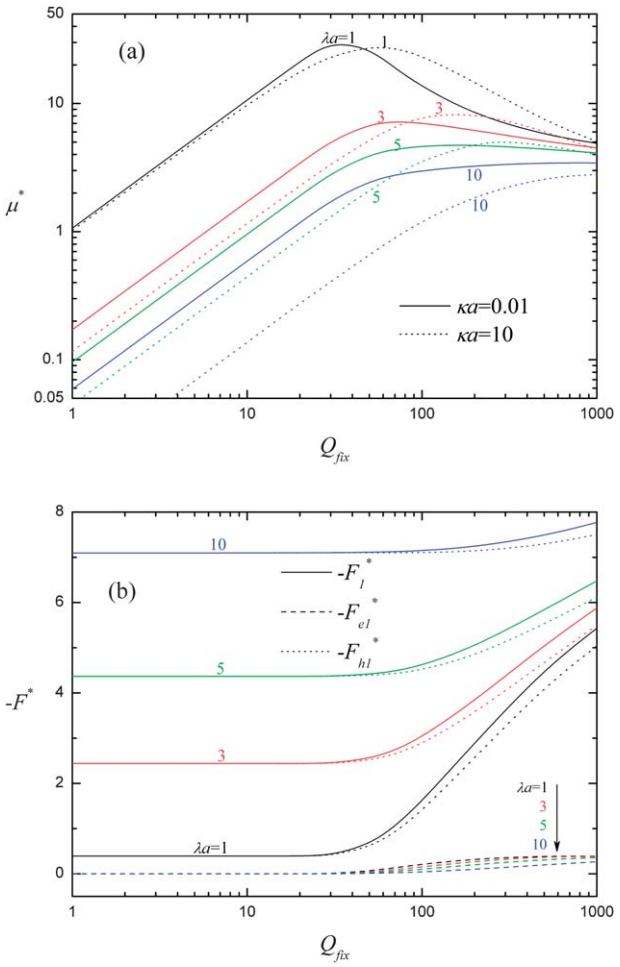

Fig. 12 Variations of the scaled electrophoretic mobility μ^*, (a), and the scaled forces in sub-problem one, $-F^*_{e1}$, $-F^*_{h1}$, and $-F^*_1$, at $\kappa a = 0.01$ in case (a), (b), as a function of Q_{fix} at various combinations of λa and κa at $\Lambda = 0.5$.

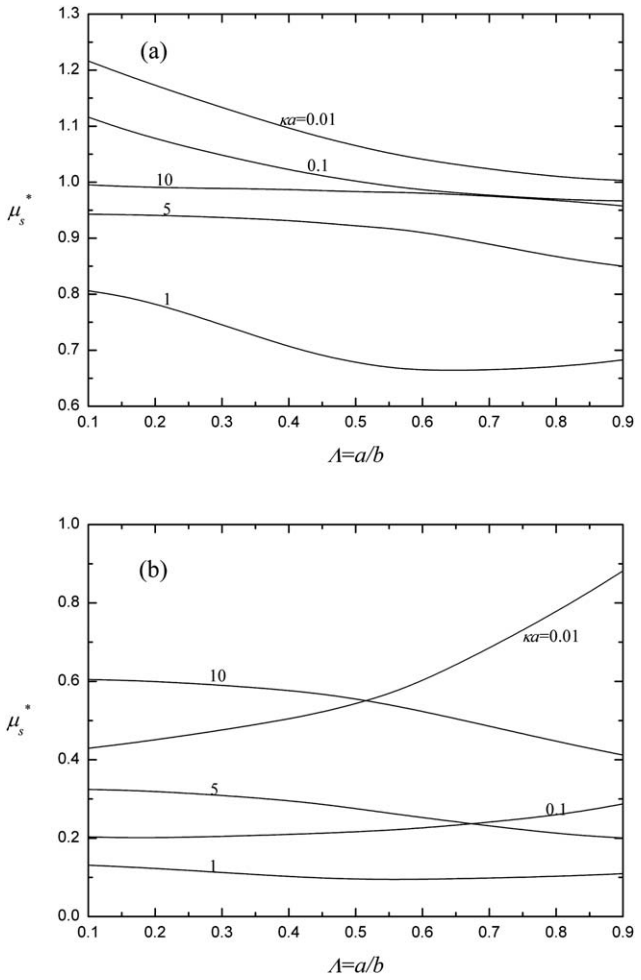

Fig. 13 Variations of the rescaled electrophoretic mobility μ^*_s as a function of Λ for various values of κa at $Q_{fix} = 10$, (a), and $Q_{fix} = 50$, (b).

relaxation effect arising from the moving of the electrolyte fluid in sub-problem one. Therefore, as illustrated in Fig. 12(b), because the strength of the relaxation electric field decreases with increasing λa, so is $|F^*_{e1}|$, yielding a decrease in the rate of both $|F^*_{h1}|$ and $|F^*_1|$ with increasing Q_{fix}. We conclude that if λa is not too large, then the larger the λa the larger is the $Q_{fix,c}$ required to overcome the relaxation effect. Note that μ^*_c decreases with increasing λa. This is because the larger the λa the larger the hydrodynamic drag force is.

3.7 Influence of pore size Λ

The influence of the pore size (or the boundary effect), measured by the parameter Λ ($= a/b$), on the rescaled electrophoretic behavior of a polyelectrolyte μ^*_s is illustrated in Fig. 13. It is interesting to note that the behavior of μ^*_s as Λ varies depends largely upon the levels of Q_{fix} and κa. At a small Q_{fix}, that is, the shielding effect is insignificant, if κa is either sufficiently small or sufficiently large, μ^*_s decreases with increasing Λ, and if κa takes a medium large value (=1), then μ^*_s has a local minimum. However, at a large Q_{fix}, that is, the shielding effect is significant or the counterion condensation occurs, if κa is small, μ^*_s increases with increasing Λ; if κa takes a medium large value (= 1), μ^*_s has a local minimum; if κa is large, then μ^*_s decreases with increasing Λ. The result μ^*_s decreases with increasing Λ can be explained by the fact that the larger the Λ the more significant the boundary effect is and, therefore, the smaller the mobility. However, as μ^*_s increases with increasing Λ and μ^*_s has a local minimum as Λ varies has not been reported previously in similar electrophoresis problems. These can be explained by the fact that at a large Q_{fix}, if κa is small, then the larger Λ the more serious the overlapping of the double layer of the polyelectrolyte with the pore is. Therefore, the larger Λ is the greater the amount of coions compressed into the polyelectrolyte is, making both the shielding effect (or counterion condensation) and the effect of DLP less significant, which has the effect of increasing the electrical driving force. If this factor is more significant than that of the increase in the hydrodynamic force with increasing Λ, then μ^*_s increases with increasing Λ.

4. Conclusions

We extend the results in the literature for the electrophoresis of rigid and soft particles to the case of an entirely porous particle

under the conditions where the boundary effect can be significant by adopting a spherical polyelectrolyte in a cylindrical pore as the model system. Due to the effect of counterion condensation, the electrophoretic behavior of the polyelectrolyte can be different both quantitatively and qualitatively from those of the corresponding rigid and soft particles. That behavior is also influenced significantly by the double layer polarization and the electroosmotic retardation flow coming from the unbalanced amount of counterions in the double layer. The general electrophoretic behavior of the polyelectrolyte can be summarized as follows: (a) if the scaled fixed charge density of the polyelectrolyte, measured by Q_{fix}, is small, its scaled electrophoretic mobility, μ^*, decreases with increasing double layer thickness, measured by κa. On the other hand, if Q_{fix} is large, then because the effect of double layer polarization is significant, μ^* shows a local minimum as κa varies. These results are consistent with the experimental observations in the literature. However, if the scaled friction coefficient of the polyelectrolyte, λa, is sufficiently large, that local minimum disappears and μ^* becomes decrease with increasing κa, which has not been reported previously in similar electrophoresis problems. This implies that the electrophoretic behavior of a polyelectrolyte depends largely on its physical properties such as Q_{fix} and λa. (b) Due to the effects of counterion condensation and double layer polarization, μ^* has a local maximum as Q_{fix} varies. If the double layer is sufficiently thick, these two effects are significant, both the local maximum of μ^*, μ_c^*, and the corresponding critical value of Q_{fix}, $Q_{fix,c}$, decrease with increasing κa. In addition, both μ_c^* and $Q_{fix,c}$ correlate positively with the degree of significance of the boundary effect. However, if the double layer is sufficiently thin, then both μ_c^* and $Q_{fix,c}$ increase with increasing κa and correlate negatively with the degree of significance of the boundary effect. If κa is sufficiently large, then the presence of the local maximum in μ^* is mainly due to the fact that the polarization effect dominates. In addition, if λa is large, regardless of the thickness of double layer, $Q_{fix,c}$ increases but μ_c^* decreases with increasing λa. (c) The competition between the hydrodynamic drag and the electrical driving force, both increase with increasing degree of significance of the boundary effect, making the electrophoretic behavior of the polyelectrolyte depend largely on Q_{fix}, κa, and how significant that effect is. For example, if Q_{fix} is large and κa is small, because the effects of the counterion condensation and the double layer polarization are alleviated by the presence of the boundary the electrophoretic mobility of the polyelectrolyte either increases or has a local minimum as the degree of significance of the boundary effect increases. This behavior has not been observed for rigid and soft (or composite) particles, where the presence of the boundary has the effect of retarding the movement of a particle, in general.

Notation

a	radius of polyelectrolyte (m)
b	radius of cylindrical pore (m)
D_j	diffusivity of ionic species j (m^2 s^{-1})
e	elementary charge (C)
$\mathbf{e}_z$	unit vector in z-direction (–)
E	strength of applied electric field (V m^{-1})
$E^* = E/E_{ref}$	scaled E (–)
$E_{ref} = \phi_{ref}/a$	reference strength of applied electric field (V m^{-1})
$\mathbf{E}$	applied electric field (V m^{-1})
f_1, f_2	proportional constant (–)
F_{ei}	z-component of $\mathbf{F_e}$ in sub-problem i (N)
$\mathbf{F_e}$	electrical force acting on polyelectrolyte (N)
F_{hi}	z-component of $\mathbf{F_h}$ in sub-problem i (N)
$\mathbf{F_h}$	hydrodynamic force acting on polyelectrolyte (N)
$F^*_{hi,s} = F^*_{hi(v),s} + F^*_{hi(p),s}$	rescaled form of F_{hi} defined by eqn (29) (–)
$F^*_{hi(v),s}$	rescaled form of viscous component of F_{hi} defined by eqn (30) (–)
$F^*_{hi(p),s}$	rescaled form of pressure component of F_{hi} defined by eqn (31) (–)
$F_i = F_{ei} + F_{hi}$	magnitude of $\mathbf{F_i}$ (N)
$\mathbf{F_i}$	total force acting on polyelectrolyte in z-direction in sub-problem i (N)
g_j	hypothetical perturbed potential associated with ionic species j (V)
$h(r,z)$	unit step region function
$h(r,z) = 0$	for the liquid phase outside polyelectrolyte
$h(r,z) = 1$	inside polyelectrolyte (–)
$\mathbf{I}$	unit tensor (–)
j	index of ionic species (–)
k_B	Boltzmann constant (J K^{-1})
n	magnitude of unit normal vector $\mathbf{n}$ (–)
n_z	z-component of unit normal vector $\mathbf{n}$ (–)
n_j	number concentration of ionic species j(#/m^3)
n_{j0}	bulk number concentration of ionic species j (#/m^3)
$\mathbf{n}$	unit outer normal vector on particle surface (–)
p	pressure of fluid phase (Pa)
$Pe_j = \varepsilon(\phi_{ref})^2/\eta D_j$	electric Peclet number of ionic species j (–)
$Q_{fix} = \rho_{fix}a^2/\varepsilon\phi_{ref}$	scaled fixed charged density of polyelectrolyte (–)
r	radial coordinate (m)
S	surface (area) of polyelectrolyte (m^2)
t	magnitude of unit tangential vector $\mathbf{t}$ (–)
t_z	z-component of unit tangential vector $\mathbf{t}$ (–)
$\mathbf{t}$	unit tangential vector on particle surface (–)
T	absolute T/K
$\mathbf{T}$	matrix transpose (–)
u_n	normal component of fluid velocity on particle surface (m s^{-1})
u_t	tangential component of fluid velocity on particle surface (m s^{-1})
$\mathbf{u}$	velocity of fluid phase relative to polyelectrolyte (m s^{-1})
U_p	z-component of polyelectrolyte velocity (m s^{-1})
$U_{ref} = [\varepsilon(\phi_{ref})^2/\eta a]$	reference particle velocity (–)
z	axial coordinate (m)
z_j	valence of ionic species j (–)
z_1	valence of cations (–)
z_2	valence of anions (–)

$\alpha = -z_2/z_1$	(-)
$\delta\phi$	perturbed potential arising from applied electric field (V)
∇	gradient operator (m^{-1})
∇^2	Laplace operator (m^{-2})
ε	permittivity of liquid phase ($C^2\ N^{-1}\ m^{-2}$)
ϕ	total electrical potential (V)
ϕ_e	equilibrium potential (V)
$\phi_{ref} = k_BTIez_1$	reference potential (V)
γ	hydrodynamic frictional coefficient of polyelectrolyte (kg $m^{-3}\ s^{-1}$)
η	viscosity of liquid phase (kg $m^{-1}\ s^{-1}$)
κ	$= [\sum_{j=1}^{2} n_{j0}(ez_j)^2/\varepsilon\, k_BT]^{1/2}$, reciprocal Debye length (m^{-1})
κa	scaled double layer thickness (–)
$\lambda^{-1} = (\eta/\gamma)^{1/2}$	softness parameter of polyelectrolyte (m)
λa	scaled friction coefficient of polyelectrolyte (–)
μ	electrophoretic mobility ($m^2\ V^{-1}\ s^{-1}$)
μ^*	scaled electrophoretic mobility defined in eqn (25) (–)
μ_s^*	rescaled electrophoretic mobility defined in eqn (28) (–)
θ	angular coordinate (–)
ρ	space charge density of mobile ions ($C\ m^{-3}$)
ρ_{fix}	fixed charge density of polyelectrolyte ($C\ m^{-3}$)
$\boldsymbol{\sigma}^{\mathbf{E}}$	Maxwell stress tensor ($N\ m^{-2}$)
$\boldsymbol{\sigma}^{\mathbf{H}}$	hydrodynamic stress tensor ($N\ m^{-2}$)
ζ_w	surface potential of pore (V)
$\Delta=[\nabla\mathbf{u} + (\nabla\mathbf{u})^{\mathrm{T}}]/2$	rate of deformation tensor (s^{-1})
$\Lambda = a/b$	(–)

superscript	
*	scaled property

subscripts	
e	equilibrium property
i	index of sub-problem
s	rescaled property

prefix	
δ	perturbed property

Acknowledgements

This work is supported by the National Science Council of the Republic of China.

References

1 M. von Smoluchowski, *Z. Phys. Chem.*, 1918, **92**, 129.
2 E. Hückel, *Phys. Z.*, 1924, **25**, 204.
3 D. C. Henry, *Proc. R. Soc. London, Ser. A*, 1931, **133**, 106.
4 J. Th. G. Overbeek, *Kolloide Beihefte*, 1943, **54**, 287.
5 F. Booth, *Proc. R. Soc. London, Ser. A*, 1950, **203**, 514.
6 R. W. O'Brien and L. R. White, *J. Chem. Soc., Faraday Trans. 2*, 1978, **74**, 1607.
7 H. Ohshima, T. W. Healy, L. R. White and R. W. O'Brien, *J. Chem. Soc., Faraday Trans. 2*, 1983, **79**, 1613.
8 E. Donath and V. Pastuschenko, *Bioelectrochem. Bioenerg.*, 1979, **6**, 543.
9 I. S. Jones, *J. Colloid Interface Sci.*, 1979, **68**, 451.
10 R. W. Wunderlich, *J. Colloid Interface Sci.*, 1982, **88**, 385.
11 S. Levine, M. Levine, K. A. Sharp and D. E. Brooks, *Biophys. J.*, 1983, **42**, 127.
12 K. A. Sharp and D. E. Brooks, *Biophys. J.*, 1985, **47**, 563.
13 M. Zembala, *Adv. Colloid Interface Sci.*, 2004, **112**, 59.
14 J. J. López-García, C. Grosse and J. Horno, *J. Colloid Interface Sci.*, 2003, **265**, 327.
15 J. J. López-García, C. Grosse and J. Horno, *J. Colloid Interface Sci.*, 2003, **265**, 341.
16 J. P. Hsu, Z. S. Chen and S. Tseng, *J. Phys. Chem. B*, 2009, **113**, 7701.
17 X. Zhang, J. P. Hsu, Z. S. Chen, L. H. Yeh, M. H. Ku and S. Tseng, *J. Phys. Chem. B*, 2010, **114**, 1621.
18 D. A. Saville, *J. Colloid Interface Sci.*, 2000, **222**, 137.
19 R. J. Hill, D. A. Saville and W. B. Russel, *J. Colloid Interface Sci.*, 2003, **258**, 56.
20 E. Lee, K. T. Chou and J. P. Hsu, *J. Colloid Interface Sci.*, 2004, **280**, 518.
21 E. Lee, Y. P. Tang and J. P. Hsu, *Langmuir*, 2004, **20**, 9415.
22 W. L. Cheng, Y. Y. He and E. Lee, *J. Colloid Interface Sci.*, 2009, **335**, 130.
23 H. Ohshima, *J. Colloid Interface Sci.*, 1994, **163**, 474.
24 H. Ohshima, *J. Colloid Interface Sci.*, 2000, **228**, 190.
25 H. Ohshima, *Electrophoresis*, 2006, **27**, 526.
26 A. Y. Grosberg, T. T. Nguyen and B. I. Shklovskii, *Rev. Mod. Phys.*, 2002, **74**, 329.
27 J. F. L. Duval, K. J. Wilkinson, H. P. van Leeuwen and J. Buffle, *Environ. Sci. Technol.*, 2005, **39**, 6435.
28 J. J. Lietor-Santos and A. Fernandez-Nieves, *Adv. Colloid Interface Sci.*, 2009, **147**, 178.
29 M. Ciszkowska and M. D. Guillaume, *J. Phys. Chem. A*, 1999, **103**, 607.
30 K. Ogawa, A. Nakayama and E. Kokufuta, *J. Phys. Chem. B*, 2003, **107**, 8223.
31 J. J. Hermans, *J. Polym. Sci.*, 1955, **18**, 527.
32 J. J. Hermans and H. Fujita, *K. Nederl. Akad. Wet. Proc. Ser. B*, 1955, **58**, 182.
33 H. C. Brinkman, *Appl. Sci. Res.*, 1947, **1**, 27.
34 P. Debye and M. Bueche, *J. Chem. Phys.*, 1948, **16**, 573.
35 J. Th. G. Overbeek and D. Stigter, *Recl. Trav. Chim. Pays-Bas*, 1956, **75**, 543.
36 N. Imai and K. Iwasa, *Isr. J. Chem.*, 1973, **11**, 223.
37 I. Noda, M. Nagasawa and M. Ota, *J. Am. Chem. Soc.*, 1964, **86**, 5075.
38 Y. Y. He and E. Lee, *Chem. Eng. Sci.*, 2008, **63**, 5719.
39 H. J. Keh and J. L. Anderson, *J. Fluid Mech.*, 1985, **153**, 417.
40 A. A. Shugai and S. L. Carnie, *J. Colloid Interface Sci.*, 1999, **213**, 298.
41 J. P. Hsu, L. H. Yeh and S. J. Yeh, *J. Phys. Chem. B*, 2007, **111**, 12351.
42 A. L. Zydney, *J. Colloid Interface Sci.*, 1995, **169**, 476.
43 J. P. Hsu and L. H. Yeh, *Langmuir*, 2007, **23**, 8637.
44 J. P. Hsu, M. H. Ku and C. Y. Kao, *J. Colloid Interface Sci.*, 2004, **276**, 248.
45 C. Ye, X. Xuan and D. Li, *Microfluid. Nanofluid.*, 2005, **1**, 234.
46 J. P. Hsu and Z. S. Chen, *Langmuir*, 2007, **23**, 6198.
47 S. Z. Qian, S. W. Joo, W. S. Hou and X. Zhao, *Langmuir*, 2008, **24**, 5332.
48 J. P. Hsu and C. Y. Kao, *J. Phys. Chem. B*, 2002, **106**, 10605.
49 H. Liu, H. Bau and H. Hu, *Langmuir*, 2004, **20**, 2628.
50 J. P. Hsu and M. H. Ku, *J. Colloid Interface Sci.*, 2005, **283**, 592.
51 S. Tseng, C. H. Cho, Z. S. Chen and J. P. Hsu, *Langmuir*, 2008, **24**, 2929.
52 J. P. Hsu and L. H. Yeh, *J. Phys. Chem. B*, 2007, **111**, 2579.
53 A. van der Wal, M. Minor, W. Norde, A. J. B. Zehander and J. Lyklema, *Langmuir*, 1997, **13**, 165.

54 G. S. Manning, *J. Phys. Chem.*, 1981, **85**, 1506.
55 G. S. Manning, *J. Phys. Chem. B*, 2007, **111**, 8554.
56 D. A. Hoagland, D. L. Smisek and D. Y. Chen, *Electrophoresis*, 1996, **17**, 1151.
57 A. Popov and D. A. Hoagland, *J. Polym. Sci., Part B: Polym. Phys.*, 2004, **42**, 3616.
58 J. Y. Gao, P. L. Dubin, T. Sato and Y. Morishima, *J. Chromatogr., A*, 1997, **766**, 233.
59 E. A. S. Doherty, R. J. Meagher, M. N. Albarghouthi and A. E. Barron, *Electrophoresis*, 2003, **24**, 34.
60 J. L. Viovy, *Rev. Mod. Phys.*, 2000, **72**, 813.
61 H. Ohshima, *Adv. Colloid Interface Sci.*, 1995, **62**, 189.
62 Y. K. Wei and H. J. Keh, *J. Colloid Interface Sci.*, 2004, **269**, 240.
63 J. P. Hsu, L. H. Yeh and M. H. Ku, *J. Colloid Interface Sci.*, 2007, **305**, 324.
64 E. Lee, J. W. Chu and J. P. Hsu, *J. Colloid Interface Sci.*, 1998, **205**, 65.
65 Y. C. Liu and H. J. Keh, *Colloids Surf., A*, 1998, **140**, 245.
66 S. Kawahata, H. Ohshima, N. Muramatsu and T. Kondo, *J. Colloid Interface Sci.*, 1990, **138**, 182.
67 K. Morita, N. Muramatsu, H. Ohshima and T. Kondo, *J. Colloid Interface Sci.*, 1991, **147**, 457.
68 O. Aoyanagi, N. Muramatsu, H. Ohshima and T. Kondo, *J. Colloid Interface Sci.*, 1994, **162**, 222.
69 J. F. L. Duval, H. J. Busscher, B. van de Belt-Gritter, H. C. van der Mei and W. Norde, *Langmuir*, 2005, **21**, 11268.
70 H. Liu and H. H. Bau, *Phys. Fluids*, 2004, **16**, 1217.
71 J. Happel and H. Brenner, *Low-Reynolds Number Hydrodynamics*, M. Nijhoff, Ed., Kluwer, Boston, MA. 1983.
72 Z. Yang, D. J. Lee and T. Liu, *J. Colloid Interface Sci.*, 2010, **214**, 220.
73 H. Fujita, *J. Phys. Soc. Jpn.*, 1957, **12**, 968.
74 T. Hoare and R. Pelton, *Polymer*, 2005, **46**, 1139.
75 A. Z. Li, L. J. Qi, H. H. Shih and K. A. Marx, *Biopolymers*, 1996, **38**, 367.
76 A. J. de Kerchove and M. Elimelech, *Langmuir*, 2005, **21**, 6462.
77 D. A. Hoagland, E. Arvanitidou and C. Welch, *Macromolecules*, 1999, **32**, 6180.
78 M. Nagasawa, A. Soda and I. Kagawa, *J. Polym. Sci.*, 1958, **31**, 439.
79 M. J. Garcia-Salinas, M. S. Romero-Cano and F. J. de Las Nieves, *J. Colloid Interface Sci.*, 2001, **241**, 280.
80 G. Chen and U. Tallarek, *Langmuir*, 2003, **19**, 10901.
81 C. P. Chiang, E. Lee, Y. Y. He and J. P. Hsu, *J. Phys. Chem. B*, 2006, **110**, 1490.